REPORT DOCUMENTATION PAGE

1a. REPORT SECURITY CLASSIFICATION Unclassified	1b. RESTRICTIVE MARKINGS None
2a. SECURITY CLASSIFICATION AUTHORITY 2b. DECLASSIFICATION/DOWNGRADING SCHEDULE	3. DISTRIBUTION/AVAILABILITY OF REPORT Approved for public release; distribution is unlimited.
4. PERFORMING ORGANIZATION REPORT NUMBER(S) NORDA Report 142	5. MONITORING ORGANIZATION REPORT NUMBER(S) NORDA Report 142
6. NAME OF PERFORMING ORGANIZATION Naval Ocean Research and Development Activity	7a. NAME OF MONITORING ORGANIZATION Naval Ocean Research and Development Activity
6c. ADDRESS *(City, State, and ZIP Code)* Ocean Science Directorate NSTL, Mississippi 39529–5004	7b. ADDRESS *(City, State, and ZIP Code)* Ocean Science Directorate NSTL, Mississippi 39529–5004
8a. NAME OF FUNDING/SPONSORING ORGANIZATION Naval Ocean Research and Development Activity 8b. OFFICE SYMBOL *(If applicable)* Code 321	9. PROCUREMENT INSTRUMENT IDENTIFICATION NUMBER
8c. ADDRESS *(City, State, and ZIP Code)* Ocean Science Directorate NSTL, Mississippi 39529–5004	10. SOURCE OF FUNDING NOS. PROGRAM ELEMENT NO. 63704N; PROJECT NO.; TASK NO.; WORK UNIT NO.
11. TITLE *(Include Security Classification)* The Impact of Satellite Infrared Sea Surface Temperatures on FNOC Ocean Thermal Analyses	
12. PERSONAL AUTHOR(S) Jeffrey D. Hawkins, John M. Harding, Juanita R. Chase,* R. Michael Clancy,** and Bonita L. Samuels**	
13a. TYPE OF REPORT Final 13b. TIME COVERED From _____ To _____	14. DATE OF REPORT *(Yr., Mo., Day)* June 1986 15. PAGE COUNT 42
16. SUPPLEMENTARY NOTATION *Computer Science Corp., NSTL, Mississippi **Fleet Numerical Oceanography Center, Monterey, California	
17. COSATI CODES FIELD / GROUP / SUB. GR.	18. SUBJECT TERMS *(Continue on reverse if necessary and identify by block number)*

19. ABSTRACT *(Continue on reverse if necessary and identify by block number)*

The Navy's global operational domain and system performance criteria place strict requirements on specifying sea surface temperatures (SST) and ocean thermal structure on many space and time scales. However, in situ observations of the ocean's temperature field are sparse and are often inaccurate. Thus, the Navy and other oceanographers have increasingly relied on remotely sensed data to fill gaps.

Infrared imagery from polar orbiting and geostationary satellites was first used from a qualitative standpoint to locate strong ocean frontal areas. Over the last 5 years, the Navy has included quantitative satellite measurements as an integral part of their SST data base. These multichannel sea surface temperatures (MCSST), 50,000–100,000 per day, far outweigh the spatial and temporal coverage of all in situ reports combined.

The MCSST data provide the Expanded Ocean Thermal Structure analysis at the Fleet Numerical Oceanography Center with highly accurate reports that span the globe. This study reveals that MCSST data significantly add to the mesoscale fronts and eddies mapping effort by tightening up strong frontal gradients and reducing the impact of noisy ship data. Higher resolution analyses are also seen to greatly aid in correctly delineating sharp ocean mesoscale features, as well as take advantage of the MCSST's 8 km by 8 km resolution.

The inclusion and proper weighting of NOAA MCSST data has upgraded the Navy's capability to map the ocean's surface thermal field. In many cases, this data has also been utilized to help infer subsurface thermal structure. This is just one example of how remotely sensed data has impacted operational Navy environmental support. Additional future sensors and space platforms will provide a variety of ocean parameters sorely needed by tactical decision makers.

20. DISTRIBUTION/AVAILABILITY OF ABSTRACT UNCLASSIFIED/UNLIMITED ☐ SAME AS RPT. ■ DTIC USERS ☐	21. ABSTRACT SECURITY CLASSIFICATION Unclassified
22a. NAME OF RESPONSIBLE INDIVIDUAL Jeffrey D. Hawkins	22b. TELEPHONE NUMBER *(Include Area Code)* (601) 688-5270 22c. OFFICE SYMBOL Code 321

DD FORM 1473, 83 APR EDITION OF 1 JAN 73 IS OBSOLETE.

DEPARTMENT OF THE NAVY
NAVAL OCEAN RESEARCH AND DEVELOPMENT ACTIVITY
NSTL, MISSISSIPPI 39529-5004

IN REPLY REFER TO

MEMORANDUM:

Ser 321/04
2 Jan 87

From: Jeff Hawkins
To: Distribution

Subj: Correction to NORDA Rept #142

Ref: (a) NORDA Rept #142, The Impact of Satellite Infrared Sea Surface Temperatures on FNOC Ocean Thermal Analyses

1. NORDA Rept #142 contained three main conclusions with regard to the impact of satellite derived sea surface temperature (SST) information.

a) The regional EOTS Gulf Stream analysis could not adequately map the mesoscale fronts and eddies without the bogus input.
b) The MCSST data allowed the analysis to retain the sharp gradients which exist in the perimeter of warm and cold core rings.
c) The MCSST data significantly reduces the noise introduced by ship observations.

2. Two figures in the report mistakenly were switched and could cause some confusion. Fig. 13(a,b,c,d) on p.21 and Fig. 14(a,b,c,d) on p. 23 should be exchanged with one another. The switch of the figures, but not the captions, will then make everything agree with the text. The new Fig. 13(a,b,c,d) shows the noise inherent in the ship obs, while Fig. 14(a,b,c,d) exhibits a much cleaner SST field benefiting from the addition of MCSST reports. This fact is seen in clearer detail when comparing Fig. 13e and Fig. 14e (the full size plots for day 5 of the test case).

3. If you have any questions, please feel free to call me at (AV 485-5270, FTS 494-5270.

Jeff Hawkins
Jeff Hawkins
Oceanographer

Distribution:
All mailing list members

Chged 2/2/87 RE

Naval Ocean Research and Development Activity
June 1986
Report 142

The Impact of Satellite Infrared Sea Surface Temperatures on FNOC Ocean Thermal Analyses

Jeffrey D. Hawkins
John M. Harding
Ocean Sensing and Prediction Division
Ocean Science Directorate

Juanita R. Chase
Computer Sciences Corporation
NSTL, Mississippi

R. Michael Clancy
Bonita L. Samuels
Fleet Numerical Oceanography Center
Monterey, California

Foreword

Our understanding of the ocean environment within which the Navy operates has increased significantly in the last decade. During this time, remote sensing of the oceans from spaceborne platforms has dramatically enhanced our capability to specify vital ocean environmental parameters on a global scale. Satellite oceanography has thus been viewed with increased optimism with regard to filling data voids that have existed since naval operations began.

Satellite sea surface temperatures were one of the first ocean parameters measured from space; thus, considerable research has been focused at refining methods to derive accurate observations. This effort has paid off to the point where NOAA operational retrievals now have an accuracy better than 0.70°C. When combined with the large number of available satellite reports, one can readily see the advantages inherent in this data source.

This report deals with the impact that infrared imagery derived products have on the Fleet Numerical Oceanography Center's ocean thermal structure analyses. Particular attention is focused on the capability of satellite retrievals to map strong frontal zones that cover mesoscale regions of interest.

A. C. Esau, Captain, USN
Commanding Officer, NORDA

Executive summary

The Navy's global operational domain and system performance criteria place strict requirements on specifying sea surface temperatures and ocean thermal structure on many space and time scales. However, in situ observations of the ocean's temperature field are sparse and are often inaccurate. Thus, Navy and other oceanographers have increasingly relied on remotely sensed data to fill the gaps.

Infrared imagery from polar orbiting and geostationary satellites was first used from a qualitative standpoint to locate strong ocean frontal areas. The Navy presently examines high resolution IR imagery to map mesoscale ocean features in a number of areas. A bogus fronts and eddies message is generated and then incorporated into the Expanded Ocean Thermal Structure (EOTS) analysis. This study clearly indicates frontal boguses are the dominant data source in the effort to effectively detect ocean features of Navy interest.

Over the last 5 years, the Navy has included quantitative satellite measurements as an integral part of their SST data base. These multichannel sea surface temperatures (MCSST), 50,000–100,000 per day, far outweigh the spatial and temporal coverage of all in situ reports combined. The MCSST data provide the EOTS analysis at the Fleet Numerical Oceanography Center with highly accurate reports that span the globe. This study reveals that MCSST data significantly add to the mesoscale fronts and eddies mapping effort by tightening up strong frontal gradients and reducing the impact of noisy ship data. Higher resolution analyses are also seen to greatly aid in correctly delineating sharp ocean mesoscale features, as well as take advantage of the MCSST's 8 km by 8 km resolution.

The inclusion and proper weighting of NOAA MCSST data have upgraded the Navy's capability to map the ocean's surface thermal field. In many cases, this data has also been utilized to help infer subsurface thermal structure. This is just one example of how remotely sensed data has impacted operational Navy environmental support. Additional future sensors and space platforms will provide a variety of ocean parameters sorely needed by tactical decision makers.

Acknowledgments

The research effort described within this report would not have been possible without a cooperative venture encompassing NORDA, FNOC and CSC. This fact is illustrated in the authorship of the report. We would also like to thank a number of other scientists and programmers who contributed significantly to the study. Pat Phoebus and Paul May (NORDA), Pam Posey (Berkeley Associates), Jim Cornelius and Ken Pollack (FNOC), Bill Pichel (NESDIS), and Fred Hamrick (CSC) helped to make this task easier and more efficient. The software now exists to repeat and expand similar case studies as circumstances warrant. The compilation of this report was directly supported by CNO OP-006 under program element 63704N, Satellite Oceanography Tactical Application Program (SOTA), A. E. Pressman, Program Manager.

Contents

I.	Introduction	1
II.	Satellite-derived SSTs	1
III.	MCSST production	2
IV.	FNOC regional SST analyses	4
V.	Impact of fronts and eddies bogus	7
VI.	Data available for regional FNOC SST analyses	9
VII.	FNOC 40-km Gulf Stream regional EOTS runs without MCSSTs	10
VIII.	FNOC 40-km Gulf Stream regional EOTS runs with MCSSTs	10
IX.	Difference fields between EOTS SST fields with/ without MCSSTs (40 km)	11
X.	FNOC 125 x 125 20-km Gulf Stream regional EOTS runs without MCSSTs	11
XI.	FNOC 125 x 125 20-km Gulf Stream regional EOTS runs with MCSSTs	11
XII.	Difference fields between EOTS SST fields with/ without MCSSTs (20 km)	12
XIII.	Effect of MCSSTs on subsurface thermal structure	12
XIV.	Summary and conclusions	12
XV.	References	13

The impact of satellite infrared sea surface temperatures on FNOC ocean thermal analyses

I. Introduction

Naval operations are highly dependent on an accurate global specification of ocean thermal structure. Knowledge of the three-dimensional ocean thermal structure is vital to the expanding antisubmarine warfare effort, as well as for optimum track ship routing and search and rescue. However, efforts to describe the ocean thermal environment have largely been restricted to only the sea surface temperature (SST) field.

The lack of in situ observations has severely hampered oceanographers in the quest to define the ocean's temperature distribution. The 200 or so expendable bathythermograph (XBT) profiles collected each day represent only a small subset of the data needed to map the mesoscale ocean features of Navy interest. These data are typically gathered along frequently travelled commercial shipping routes and leave many important ocean areas severely undersampled. Thus, it is extremely difficult to even guess at the subsurface conditions in many areas of the world.

Fortunately, our ability to map out the SST field around the globe has been marked by increasing degrees of success over the last 5–10 years. Ship SST observations transmitted in 6-hourly meteorological reports have been the mainstay of the network to monitor the ocean's surface temperature. These 4000–5000 data points per day have an RMS error of 1.5°C (Pichel, 1984) and provide adequate information in some of the North Atlantic and Pacific shipping lanes, but fall far short in most other sectors. This critical drawback has been supplanted in the last 6–7 years by satellite-derived SSTs, which have matured to the point where their accuracy makes them highly useful.

This report details recent progress within the Navy to specify the mesoscale SST fields on high-resolution regional grids. More specifically, this report demonstrates the impact of satellite-derived SSTs on the operational Fleet Numerical Oceanography Center's (FNOC) thermal structure analysis for the Gulf Stream region.

II. Satellite-derived SSTs

SSTs have been routinely obtained from infrared sensors on spaceborne platforms since 1973 (Brower et al., 1976). These early efforts (Table 1) were necessarily crude because the spectral windows were wide and were contaminated with water vapor. No viable means existed then to correct for the attenuating nature of the intervening atmosphere, resulting in SSTs that were far too cool and easily in error by 2–4°C. Rao et al. (1972) used a global data set of ship reports to obtain an RMS error of 2.5°C for SSTs produced with Improved TIROS Operational Sounder (ITOS 1) data in 1970.

These statistics remained valid through the early 1970s as the sensors slowly changed to reflect the requirement to view the ocean surface through narrower "atmospheric windows." Several years later, the thermal sensitivity of the instruments also advanced to the point where relative SSTs of 0.5°C precision (8-bit digitization) could be sensed. The launch of the Tiros-N series of polar meteorological satellites (1978) with the Advanced Very High Resolution Radiometer (AVHRR) and corresponding atmospheric sounder finally turned the tide as far as satellite-derived SSTs are concerned. By 1980, the National Oceanic and Atmospheric Administration (NOAA) had cracked the 2°C RMS barrier by using data from the sounder to estimate the amount of water vapor in the atmospheric column (McClain, 1980).

Table 1 also reflects the fact that this success was quickly followed by using a multichannel technique (via AVHRR) to get under the 1°C RMS error bar. NOAA-6 satellite data from channels 3 and 4 were combined to correct for the effects of water vapor. This combination was possible, since the two channels have different transmissivities with respect to water vapor as shown in Figure 1. This differential absorption phenomenon can be used to adjust one of the infrared temperatures upward by an amount proportional to the temperature difference between the two channels.

A distinct benefit of this technique is its pixel-by-pixel correction capabilities. The previous sounder methods assumed the atmosphere was horizontally uniform over the sounder field of view (FOV—typically 150 km). This drawback was obvious because mesoscale water vapor gradients in the FOV were simply averaged out, thereby degrading the resultant SST. Table 1 indicates that the multichannel correction has remained accurate to within 1°C since its inception and lately has reached a level near 0.6°C using multichannel SSTs (MCSSTs) from NOAA-9 compared with FGGE drifting buoys (Strong and McClain, 1985; McClain, 1986).

Table 1. Satellite SST accuracies.

Data Date	Sensor	Bias	RMS		Surface Truth	Reference
Sep 1970	ITOS 1		2.5		Ships-Global	Rao (72)
	ITOS 1		2.0		Weather Ships	"
1972	Nimbus-2		1.5		Ships	Shenk (72)
1979	Tiros-N		2.2		Global Ships	McClain (82)
1980	N6-MCSST	0.01	0.91		Buoys, XBT (69)	McClain (80)
79–80	N6-MCSST		0.60		Buoys, ships (82)	Bernstein (82)
	Ships		1.24		Buoys, ships (1000)	"
1981	N7-MCSST	0.40	0.98		Buoys (47)	Pichel
	(Ch3–4)	2.10	0.84		"	Deschamps B
		0.01	0.84		"	Bower O
						W
1981	N7-MCSST	0.72	0.51		Buoys (13)	Pichel E
	(Ch 345)	0.96	0.47		"	Deschamps R
		0.00	0.31		"	Bower
1981	N7-MCSST	0.03	0.91		Buoys, XBT (124)	McClain (81)
Nov 1981	N7 1 Ch	−0.40	1.46		Buoy (73)	Pichel (81)
	N7-MCSST	0.02	0.58		Buoy (74)	"
1981	N7-(3–4)	0.02	0.62		Buoy (74)	McClain (81)
	(4–5)	−0.03	0.63		"	"
	(345)	0.02	0.58		"	"
Dec 1981	N7-MCSST	−0.50	0.60		Binned ships (700)	Bernstein (85)
Nov 1981—	N7-MCSST	−0.03	0.60	D	Buoys (124)	McClain (82)
Apr 1982		−0.42	0.75	N	Buoys (143)	"
Mar 1982	N7-MCSST	−0.01	0.80	D	Drift buoy (51)	McClain (82)
		0.04	0.70	N	" (94)	"
		0.02	0.70	All	" (145)	"
Mar 1982	N7-MCSST	0.36	0.51		Binned Ships (700)	McClain (85)
May 1982	N7-MCSST	0.11	0.85	D	Buoys (244)	McClain
		−0.02	0.73	N	Buoys (173)	"
81–82	N7-MCSST	0.27	0.75		XBT (360)	Hilland (85)
Oct 1985	N9-MCSST	0.26	0.59	D	Drift Buoys (234)	McClain (86)
		0.12	0.44	N	Drift Buoys (110)	"
Dec 1985	N9-MCSST	0.25	0.61	D	Drift Buoys (264)	McClain (86)
		−0.10	0.50	N	Drift Buoys (160)	"

The methods used to verify satellite SSTs have changed over the years to produce better in situ reports, which are required to adequately determine MCSST capabilities. Ships within 100 km of satellite retrievals were routinely used in the early 1970s as surface truth. Only later did closer scrutiny reveal that the ship observations were only accurate to within 1.5°C (Table 1). Therefore, most efforts to validate MCSSTs have shifted to the use of buoys existing outside the high-gradient coastal waters where most fixed buoys reside. Drifting buoys from the FGGE program satisfy the criteria for highly accurate open-ocean platforms that sense the temperature close to the ocean surface ($\sim$1 m depth).

III. MCSST production

Satellite infrared SSTs are limited to cloud-free regions. This restriction can be severe because such areas as the Arctic during certain seasons, the Intertropical Convergence

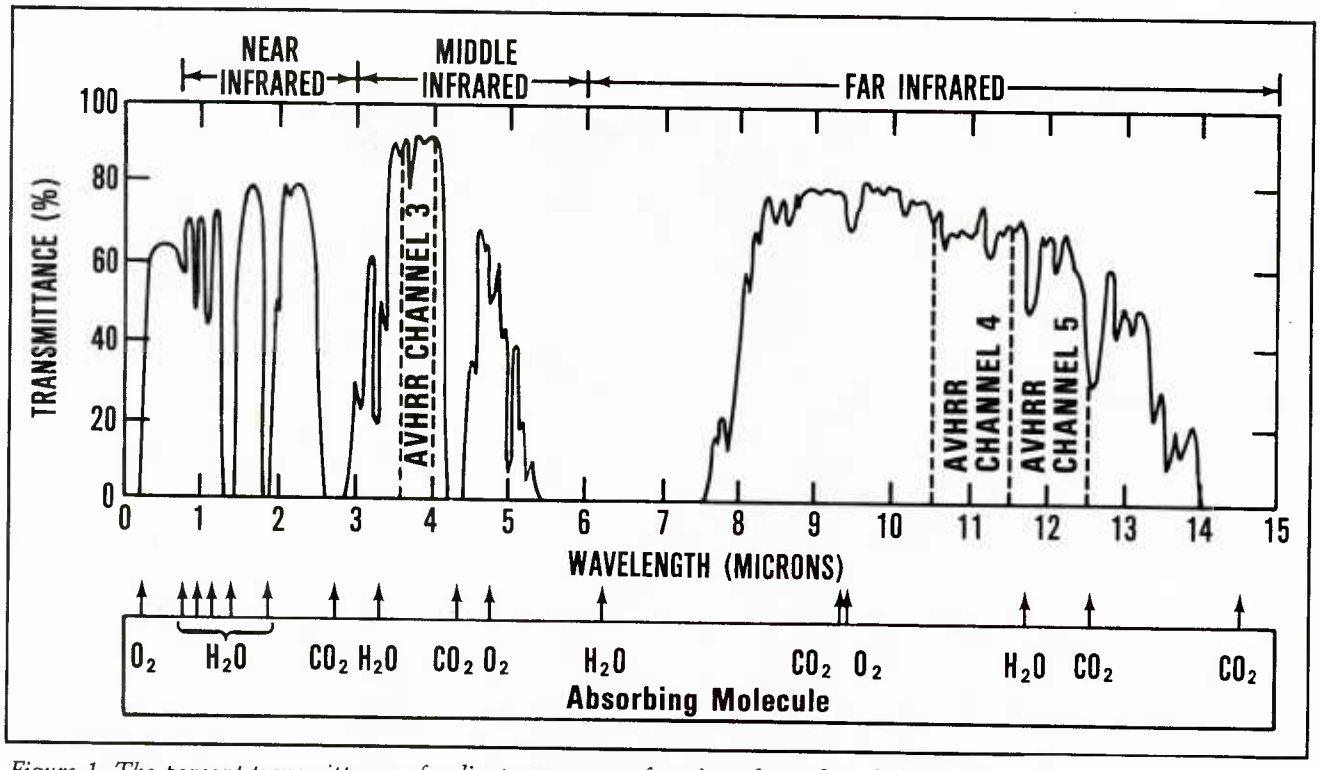

Figure 1. The percent transmittance of radiant energy as a function of wavelength for the spectral range, which includes the infrared channels on the present NOAA AVHRR (Holyer and Hawkins, 1982).

Zone, and the Eastern Pacific are persistently cloudy. The twice-daily observations provided by the NOAA polar orbiters are thus inadequate when clouds obscure a particular zone of interest. Using two polar orbiters would increase the sampling to four times/day (even more at high latitudes) and improve the chances for a cloud-free view, but must be weighed against the added processing necessary to accomplish the task. Thus, the particular application requirements and computer resources will determine which avenue is chosen.

Satellite SST algorithms do not produce a retrieval for every cloud-free pixel available. Instead, a search pattern is derived to find up to a set number of MCSSTs per given target array. Whether or not this number of observations is reached depends on the cloud cover at the particular time and location. Thus, some areas may be devoid of retrievals while others have high-density sampling. Such patterns are illustrated in Figure 2, which shows the distribution of MCSSTs in the Northern Hemisphere for 60 hours. The individual swaths of data are clearly depicted in this data display.

Even though data from all orbits are processed, Figure 2 shows a preponderence of ascending (daytime) reports and no real evidence of descending swaths. This is an artifact of the National Environmental Satellite Data and Information Service (NESDIS) processing algorithms. Nighttime data preclude the use of visible reflectance information from channel 2 and thus forces NOAA to use strict infrared uniformity tests to weed out cloud-contaminated pixels. The number of retrievals at night is thus only a fraction of those during the day, and the normal ratios are 20,000 (nighttime) to 70,000 (daytime), respectively. The lower number of nighttime MCSSTs can also be explained by the density of retrievals allowed per target array (which consists of an 11 x 11 array of Global Area Coverage—GAC 4-km data). Once the algorithm finds a 2 x 2 GAC unit array that passes all the cloud tests, it produces an MCSST and moves onto the next target array.

The daytime algorithm permits the user to select ocean regions where enhanced MCSST coverage is desired. The software enables the specification of 10° latitude-longitude boxes where either medium- (5) or high- (15) density retrievals (per 11 x 11 GAC array) can be attempted. This procedure does not ensure that these numbers will be reached, but simply states that if this number of cloud-free matchups exists, they will be used to produce SSTs. Thus, the difficulty of discerning nighttime clouds, combined with the daytime high-density zones, creates the huge difference in number of day and nighttime MCSSTs.

Figure 3 is a global chart that indicates the zones now included for medium- and high-density retrievals. These areas have been requested by a number of government/academic operational and research investigators who need more than one SST per GAC 11 x 11 array for their particular application. The Gulf Stream region was one of the first designated as a high-density sector. The Mediterranean Sea and the Kuroshio current were later added at NORDA's request, and Alaska, East Australia, South Africa, and the equatorial Atlantic and Pacific were added by NOAA through numerous appeals.

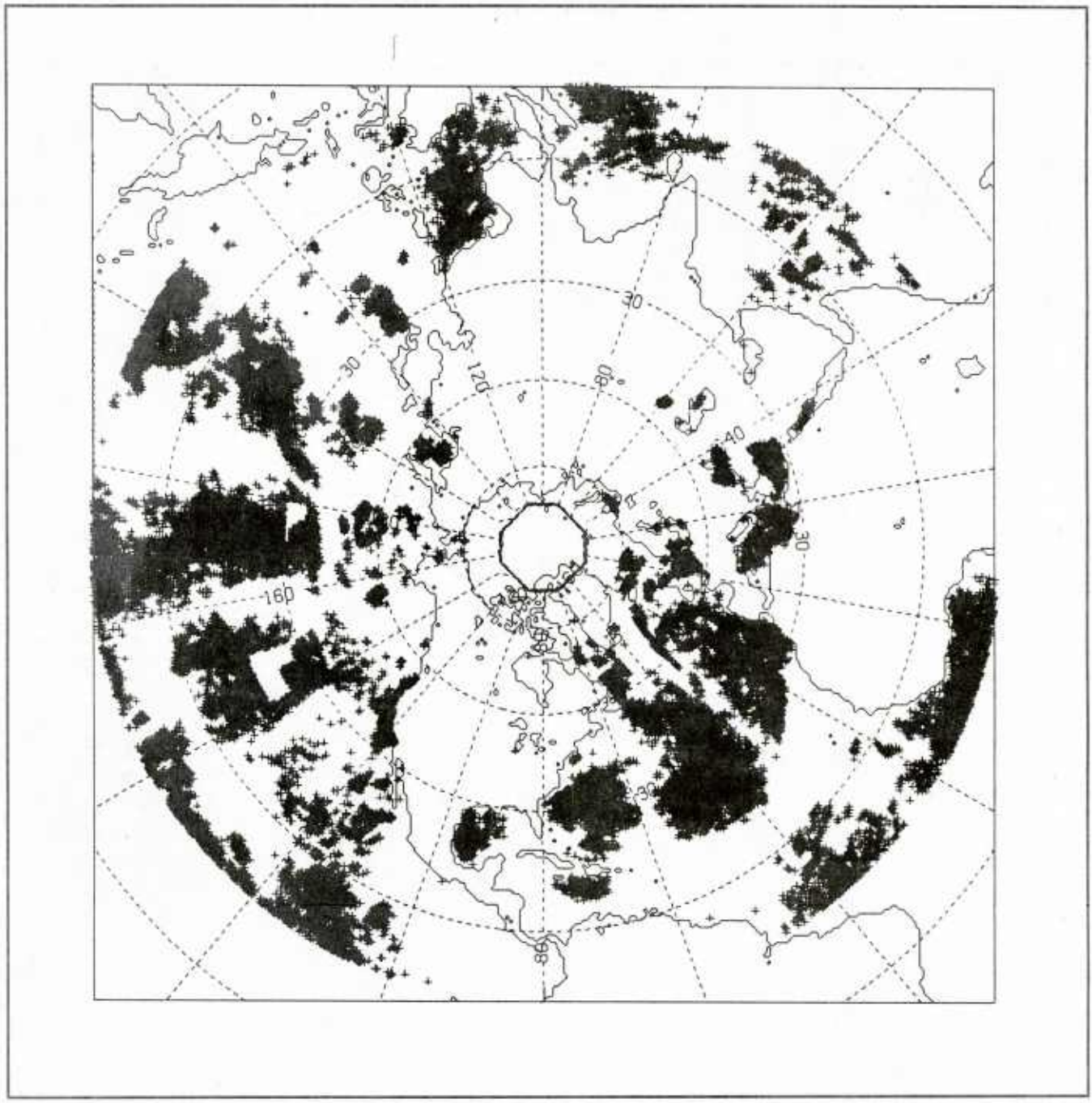

Figure 2. Data distribution plot for MCSST over the Northern Hemisphere valid 12Z 30 June 1986.

Other domains of high Navy interest will likely be added when FNOC begins producing MCSSTs within the next two years.

NESDIS MCSSTs are transmitted to FNOC once every three hours from the National Meteorological Center (NMC). These observations contain latitude, longitude, time, and SST with 0.01°C precision. This data set has been routinely received at FNOC since fall 1983. Before then, a small subset of the global data was available on the Automated Weather Network. This earlier system permitted only the transmission of one satellite SST for every 2.5° square. Therefore, prior to fall 1983, the number of reports typically averaged under 2000 globally per day. This data was beneficial to the hemispheric SST analyses, but did not have the data density necessary to significantly impact the regional analyses.

IV. FNOC regional SST analyses

FNOC generates SST analyses on two separate spatial scales, hemispheric and regional. Hemispheric versions of the Expanded Ocean Thermal Structure (EOTS) analysis are run daily for both the Northern and Southern Hemispheres as detailed in Table 2. These large-scale analyses assimilate ship, XBT,

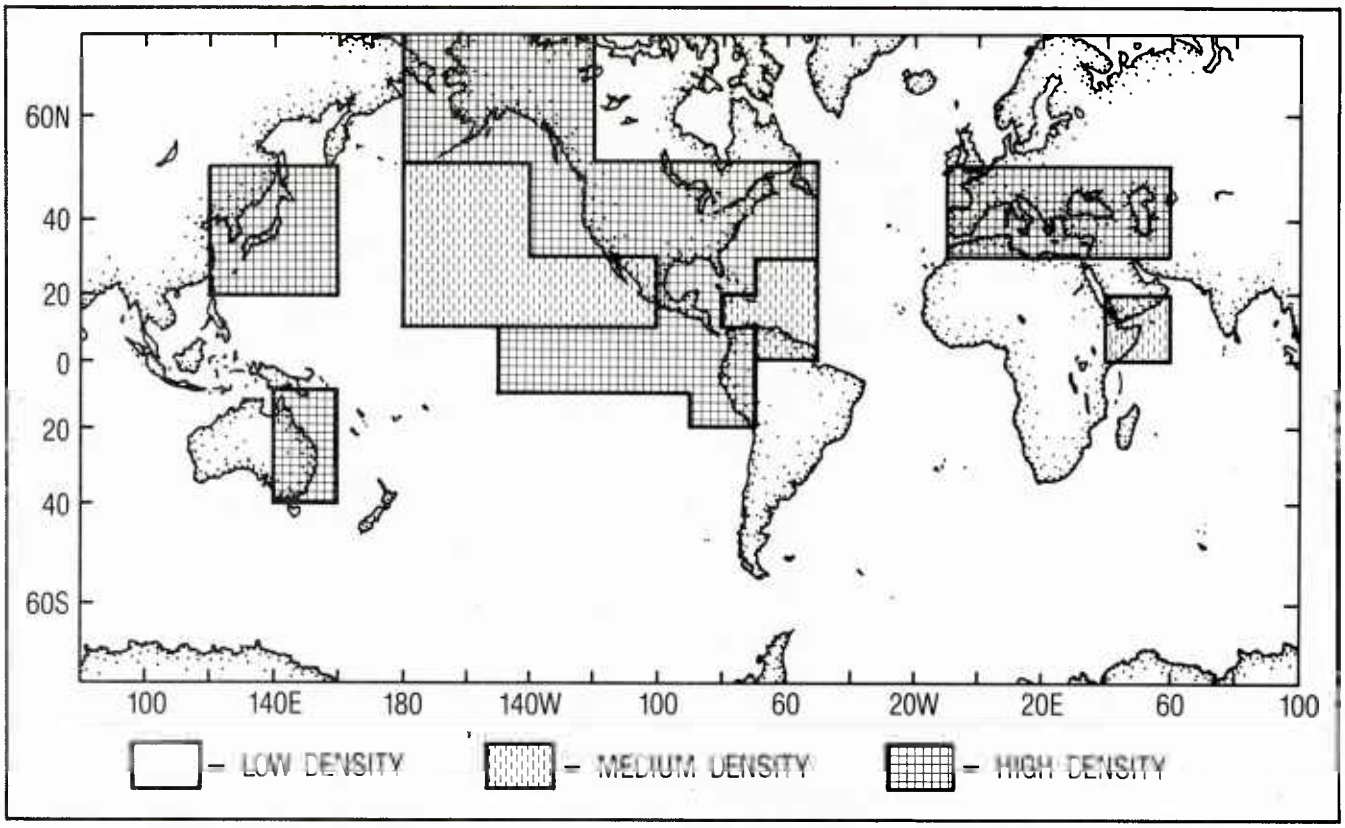

Figure 3. Global chart indicating zones where medium- (5) and high- (15) density MCSST retrievals are operationally derived by NESDIS if cloud conditions permit (courtesy Bill Pichel).

Table 2. Expanded ocean thermal structure (EOTS) analyses

Region	Resolution (km)	Schedule	SST-Bottom	SST	PLD	TEOTS
N. Hemisphere	320	2/Day	*	*		*
S. Hemisphere	320	2/Day	*	*		*
Norwegian Sea	40	Daily	*			*
W. Mediterranean	40	Daily	*			*
E. Mediterranean	40	Daily	*			*
Gulf Stream	20	Daily	*			
N. Kuroshio	32	Daily	*			
S. California	40	Daily	*			
Caribbean	32	Daily	*			
Indian Ocean	80	Daily	*			
S. China Sea	40	M,W,F,Sa		*	*	
Mid Pacific	54	Tu,Th,Su		*		
S. Kuroshio	40	Tu,Sa		*	*	
Labrador Sea	40	M,W,F,Su		*		
Iberian Sea	40	M,W,F,Su		*		

SST—Sea Surface Temperature
PLD—Primary Layer Depth
TEOTS—EOTS is cycled with TOPS forecast model

buoy, and satellite MCSST reports to map out the three-dimensional ocean thermal structure using a grid with ~320 km resolution. This assimilation is done by using the Fields by Information Blending (FIB) technique (Holl et al., 1979).

The 17 levels defined within EOTS are shown in Figure 4. By virtue of the satellite MCSSTs, the SST or top layer is easily the most accurate of the EOTS levels. The FIB technique blends data vertically, as well as horizontally, but the

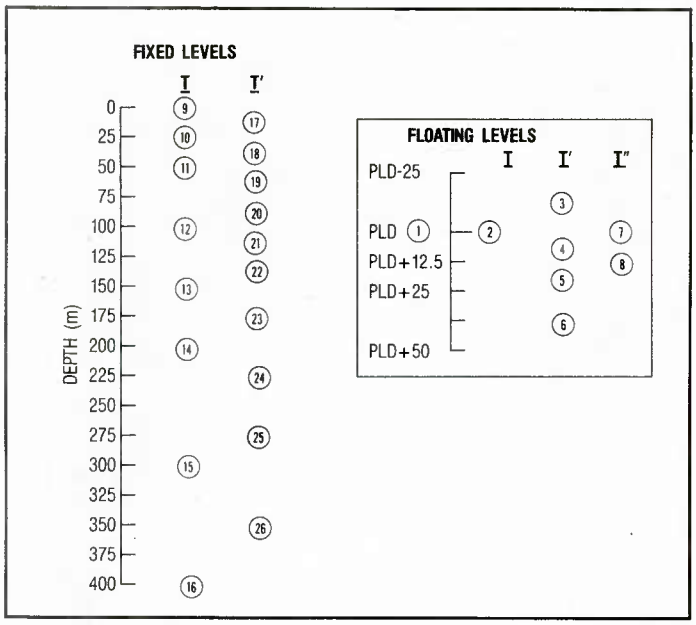

Figure 4. Levels used by EOTS analysis to specify the ocean's vertical temperature profile.

value of this approach is limited if subsurface thermal anomalies are uncorrelated (or perhaps negatively correlated) with the relatively well-observed SST anomalies. EOTS, combined with an upper-ocean thermal structure forecast model such as the Thermodynamic Ocean Prediction System (Clancy and Pollak, 1983), can help specify the variability within the surface mixed layer resulting from synoptic weather events. This cycling presently occurs operationally for the Northern and Southern Hemisphere and the eastern and western Mediterranean versions, as well as for the Norwegian Sea.

The regional EOTS analyses cover particular areas of Navy interest and utilize grid spacing that ranges from 20 km for the Gulf Stream to 80 km for the Indian Ocean regions (Table 2). To reasonably resolve a particular ocean feature, one should have 3–4 points to describe it. Thus, a 20-km grid allows us to map eddies with a diameter of about 70 km. This value is typical of many warm and cold core rings in the Gulf Stream, although sizes vary dramatically.

Many of the regional EOTS areas have high-resolution fronts and eddies bogus messages generated for them by one of the regional oceanographic centers (NEOC—Norfolk, NOCC—Guam, NOCC—Rota, Spain). Figure 5 is an example of a Gulf Stream fronts and eddies bogus derived from satellite infrared imagery available at Norfolk. This information is received at FNOC in the form of latitude-longitude pairs that depict the northern and southern wall of the Gulf Stream and the temperature gradients, plus the location and radius of eddies. This information is included in the EOTS data base along with ship, buoy, XBT, and MCSST data.

The bogus, as a heavily weighted input, tries to force the EOTS analysis to draw the front or eddy at the detected position. However, for the Gulf Stream, even 40-km regional versions are too coarse to adequately handle the bogus information. The product is not capable of retaining the sharp horizontal thermal gradients that occur along the north wall. Instead, this front is smoothed out between grid points both at and below the surface. Thus, methods have been developed to help pack the isotherms more realistically (i.e., the north wall is moved 20 nautical miles toward the cold water to keep the gradient of the current out of the core of the stream). One will note in later figures how the sharp gradient passes directly through Cape Hatteras to conform with this standard. This method introduces severe problems if the subsurface gradients are used to calculate geostrophic currents.

In light of these facts, FNOC and NORDA have been jointly working on methods to improve the ocean thermal analyses product. First, EOTS is now running operationally on a 125 x 125 grid for the Gulf Stream, Northern Kuroshio, and Caribbean areas, providing resolutions of 20, 32 and 32 km, respectively. Second, NORDA is working on replacing EOTS with an optimum interpolation-based product designated as the Optimum Thermal Interpolation System—OTIS (Innis, 1983 and 1985). Improvements expected from the replacement of EOTS with OTIS will be briefly covered later. The remainder of this report details the impact of satellite MCSSTs on the Gulf Stream regional EOTS using both the 63 x 63 and 125 x 125 grids during the week of 16 July 1985. Note that the Gulf Stream operational EOTS changed from 63 x 63 (40 km) to 125 x 125 (20 km) in the summer of 1985, and more recently the cold water shift of the north wall has been removed.

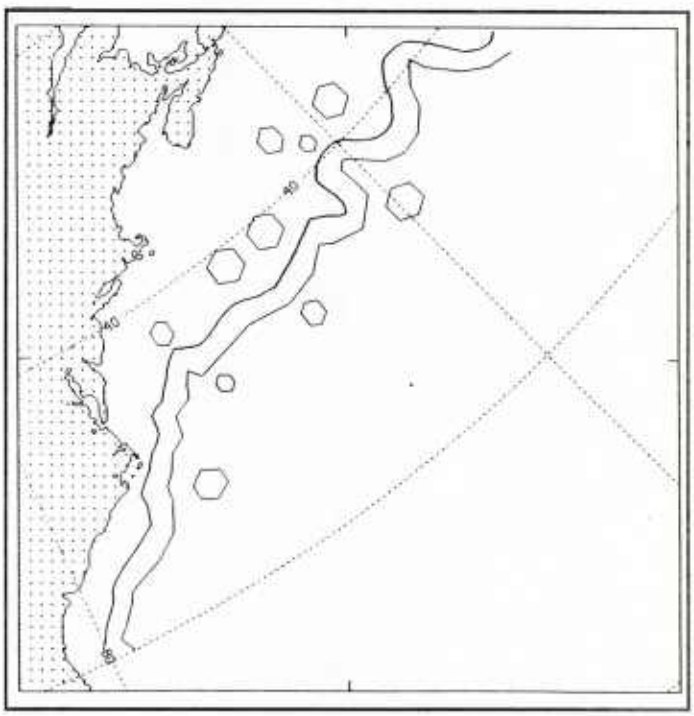

Figure 5. Plot of the EOTS bogus message depicting the location of the north and south wall of the Gulf Stream, as well as warm and cold core rings. Data is derived mainly from infrared imagery interpreted at NEOC and valid for 19 July 1985.

V. Impact of fronts and eddies bogus

Climatological SST values are incorporated into the EOTS analyses with increasing weight when data density becomes poor. If MCSST, ship, XBT, buoy, and/or IR bogus data does not exist in a given area for a few days, the analysis reverts to climatology. This methodology tends to smooth out the temperature field, especially below the surface. This tendency can be offset in part by the operational coupling of the TOPS model with EOTS. The coupling allows atmospheric forcing (winds and heat fluxes) to modify the ocean thermal structure and becomes increasingly important in data void regions. This coupling, however, does not currently exist operationally for the Gulf Stream region.

Figure 6 illustrates the SST climatology valid for 16 July. This field was generated by interpolating between monthly averages for the day in question. The test cases described in the next section used this SST field as a first guess for the analysis. The smooth pattern is completely void of any fronts and eddies and represents the average of a large number of measurements taken over many years. The first inclusion of new data must then modify this field to accurately represent the current conditions. This requires an adequate distribution of data and is helped immensely by the NEOC fronts and eddies bogus.

The EOTS analysis scheme has been formulated to accept fronts and eddies positions derived primarily by human interpretation of infrared imagery. These bogus messages are produced once per week for the Gulf Stream area and also include any additional information resulting from ship, buoy, and XBT reports. In practice, the vast majority of the data used to derive the bogus comes directly from the Advanced Very High Resolution Radiometer (AVHRR) imagery.

This section describes a test evaluating the impact of the bogus fronts and eddies on the final Gulf Stream EOTS SST analysis. Offline parallel EOTS runs were made with/without the bogus after starting from climatology on 4 August 86 (looks very similar to Fig. 6). Figure 7 shows the NEOC generated Gulf Stream bogus valid for day five of the test case. Three warm and three cold core eddies are adjacent to a Gulf Stream front that has several large meanders. Note the varying size of the eddies and the fact several are quite close to the Gulf Stream and may be absorbed at any time.

All available MCSST, ship, buoy, and XBT data were input to both parallel runs with/without the bogus. Figure 8, the data distribution XBTs, ship/buoys, and MCSSTs on 8 August 86 indicates the typical distribution for each of these data sources. The number of XBTs averages between 10–30 (48 hour period), ships/buoys average about 250–275 (72 hour period) after taking into account many fixed buoys report every 1–3 hours, and MCSSTs range from 1,000–3,000 (60 hour period). The data void regions in the MCSST plot are filled in during the five day test case that runs from 4 August to 8 August 86.

Figure 9a represents the EOTS SST pattern after five days with one iteration per day at 12Z. This series of runs without the fronts and eddies bogus attempts to define the north wall of the Gulf Stream and the shelf-slope front, but the end result is poor at best. Some areas of the front are better than others and reflect the availability of data to define certain features.

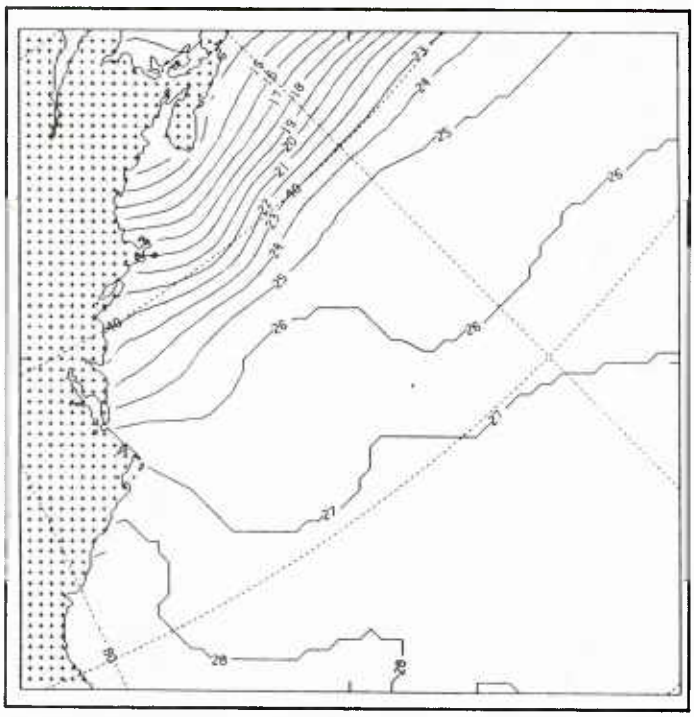

Figure 6. SST climatology for the Gulf Stream region valid for 16 July and mapped to the FNOC 63 x 63 40-km grid.

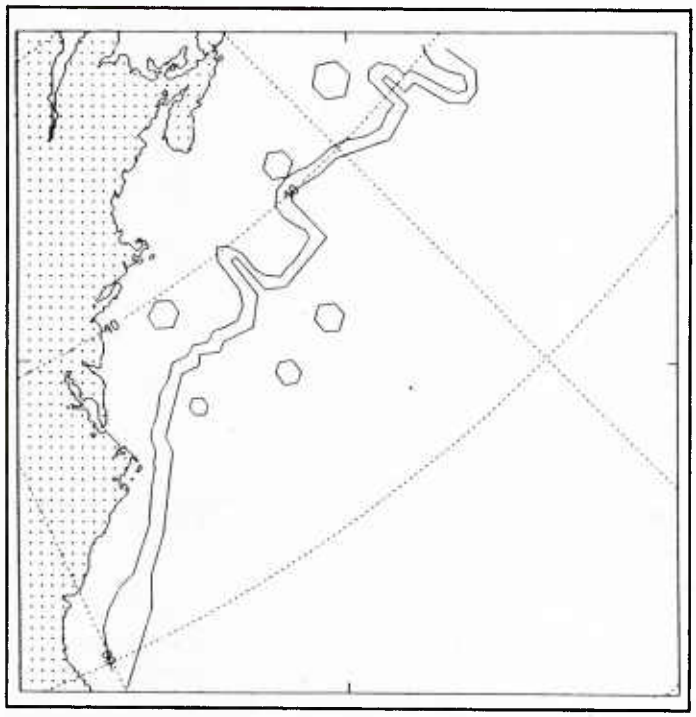

Figure 7. NEOC fronts and eddies Gulf Stream bogus valid at 12Z 8 August 86.

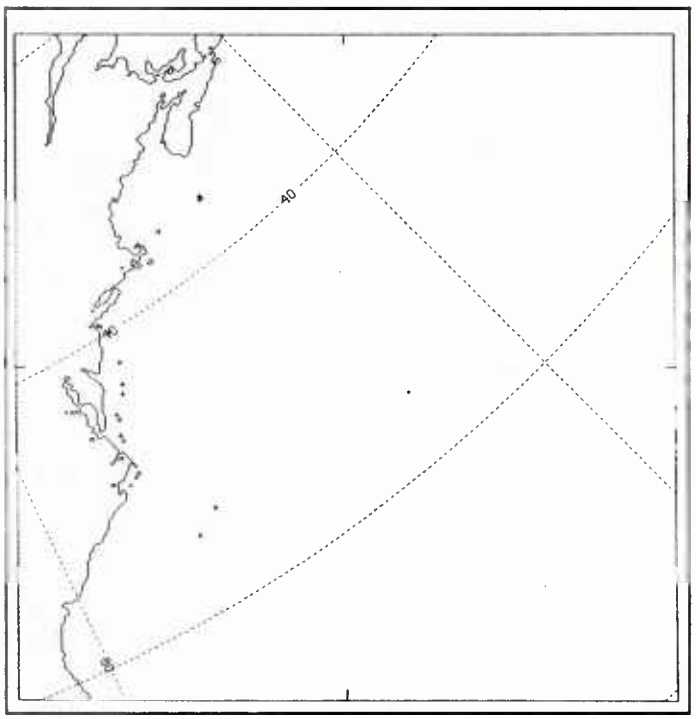

Figure 8a. Distribution of XBT observations resident in FNOC files between 12Z 6 August and 8 August 86.

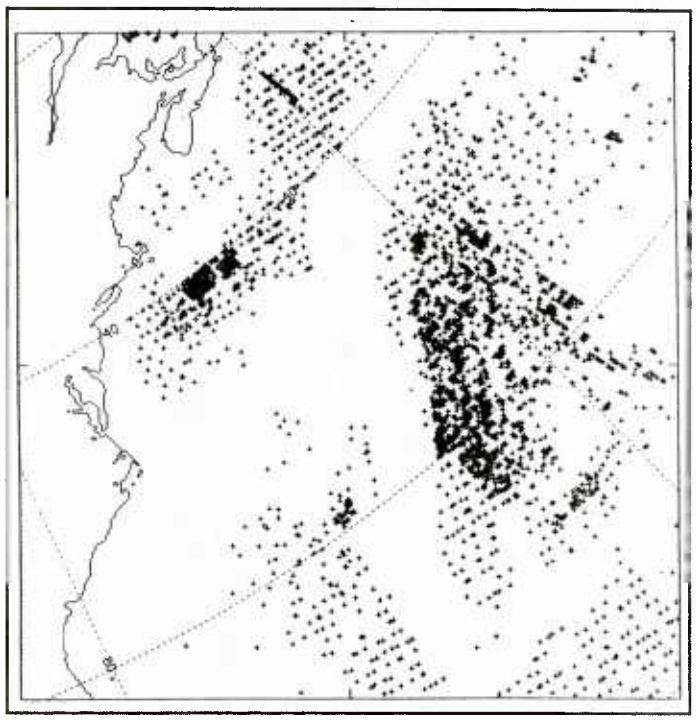

Figure 8c. Distribution of MCSST observations resident in FNOC files between 00Z 6 August and 12Z 8 August 86.

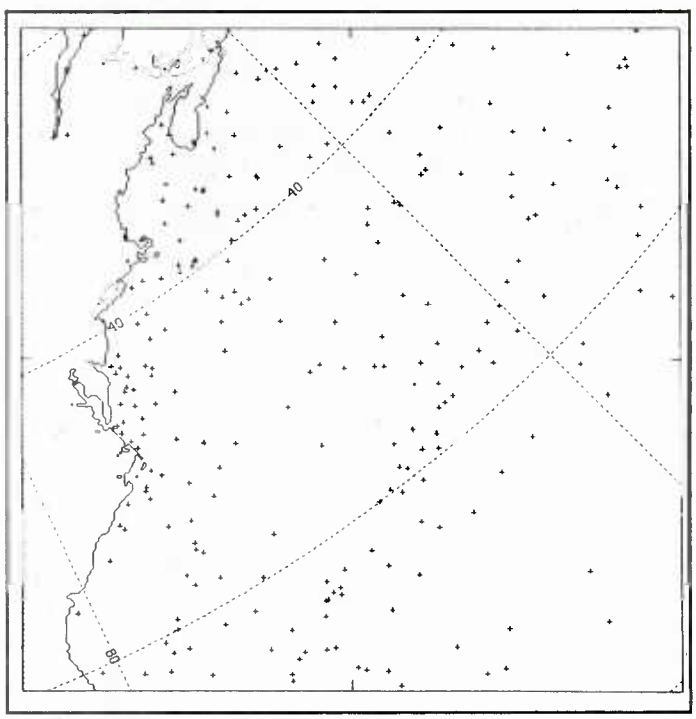

Figure 8b. Distribution of ship/buoy observations resident in FNOC files between 12Z 5 August and 8 August 86.

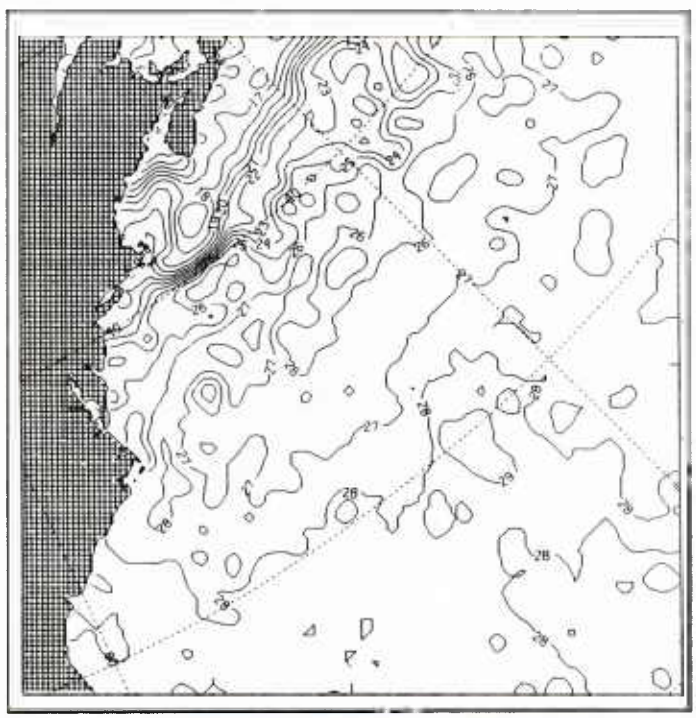

Figure 9a. Gulf Stream regional EOTS SST Field (without bogus input) for day five (8 August 86) of test case.

However, over the five day cycling of this test run without the bogus, EOTS does not produce a Gulf Stream or eddy field that is realistic. This product would be unacceptable in terms of defining the tactically significant features of Navy interest.

The parallel run with bogus input (8 August 86, Figure 9b) represents a radical change in the Gulf Stream region. The north and south wall are relatively well defined in this 20 km resolution analysis and the eddies stand out dramatically against the background slope and Sargasso Sea waters. The warm eddies

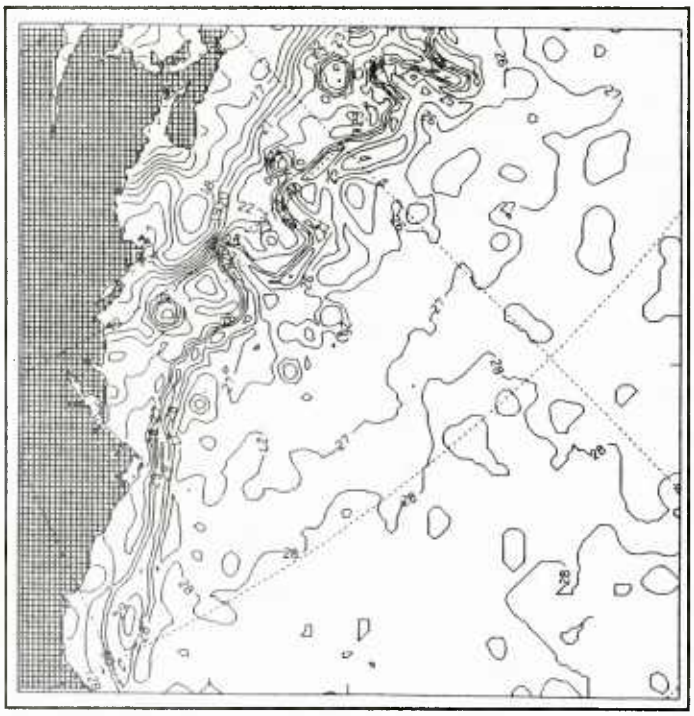

Figure 9b. Gulf Stream regional EOTS SST field (with bogus input) for day five (8 August 86) of test case.

are particularly evident since their SST gradient with the ambient slope waters is still quite large. The cold eddies in the Sargasso Sea have lost most of their surface thermal expression in August and are harder to locate in IR imagery and any subsequent SST field. Minor differences occur in the two fields outside the area of bogus influence since the two cases are run back to back and the data files sometimes are updated slightly between runs.

The fronts and eddies NEOC bogus thus plays a major role in the present EOTS analysis methodology. The boguses provide the primary means of identifying these features. The XBT, ship/buoy, and MCSST data can not by themselves define the fronts and eddies when assimilated via the FIB technique. In response to this fact, NORDA and FNOC are working on an optimum interpolation technique which we hope will more accurately reflect the capabilities of all data sources to map the mesoscale features of interest.

The boguses can provide a false sense of security when one realizes that IR imagery can often times be cloud covered in the Gulf Stream for several days at a time. Therefore, the analyst can have very limited data to work with. NORDA is presently developing the methodology and software to merge GEOSAT altimeter sea surface dynamic heights with IR data to alleviate some of the cloud limitations inherent with infrared imagery.

It should be noted that subjective human interpretation differs from analyst to analyst and requires a certain lengthy learning curve before a person becomes qualified. The fronts and eddies may also move appreciably in the one week time frame between bogus updates. This is especially true when the front is unstable and eddies are in the process of being shed or absorbed by the Gulf Stream. Bogus messages should therefore be generated as conditions warrant.

The following section details another case study where the impact of just the MCSST data is examined. The bogus information is included in all the runs, but the MCSST data is withheld in one case and included in another to judge the effect they have on the EOTS analyses. Data distribution is critical in this study and thus shown in more detail than in the first study on the impact of boguses.

VI. Data available for regional FNOC SST analyses

The hemispheric EOTS analyses cover such large domains that the number of observations available for input seem huge (i.e., 60,000–70,000 MCSSTs, 4000–5000 ship observations and 200 XBTs per day). However, the benefit inherent in the superior MCSST data distribution is lost in the 320-km gridding. The following test attempts to determine the impact that satellite SSTs have on the finer resolution (40 km and 20 km) Gulf Stream analyses. As background information, we present examples of the data available for assimilation into the analyses.

The regional EOTS system uses 48 hours of XBTs, 72 hours of ship data, and 60 hours of MCSSTs. These varying time windows for data entry were selected after considering the number and distribution of observations and the typical delays for receiving each type of report. Figure 10 is a plot of the Gulf Stream XBT data distribution (48 hours of data) for each of the five EOTS runs used in this test set. The 7–20 reports shown in Figures 10a–e offer very poor coverage and usually come from no more than four or five ships. The amount of new subsurface information is obviously limited. (Note: The data base used for this study does not include classified XBT reports.)

SSTs available from a combination of ships and buoys offer much improved coverage for the Gulf Stream region. Figures 11a–e reveal that 800–900 reports are available for any given 72-hour time frame. This total is heavily biased with buoy measurements because NOAA has numerous platforms in the area, many of which report every 1–3 hours. Thus, it is entirely possible to have 72 SSTs from the same fixed station included in the EOTS data base. The ratio of ship measurements to buoy reports is roughly 250 to 600, which means that the actual number of SSTs available for the analysis is closer to 275 ship/buoy reports, since only the latest buoy observation is utilized.

In contrast to the XBTs and ships/buoys, over 2,000 MCSSTs in any given 60-hour span can be ready for regional

EOTS use (more recent data checks indicate this value can approach 6,000). Figures 12a–e depict the distribution of satellite infrared SSTs for the five test days and clearly show wide variability from day to day. Figure 12a contains a large gap in the middle of the grid, Figures 12b, c, e show areas saturated with high-density retrievals, and Figure 12d has one swath of data punctuated with cloud cover. Each coverage chart is directly related to the meteorological conditions prevalent at the time and exhibit the potential feast-or-famine nature of infrared SSTs.

It should be noted that due to a 10–14 hour delay in processing and disseminating the MCSSTs from NESDIS-NMC-FNOC, the 60-hour window is really 48 hours. In the future, when MCSSTs are produced locally from FNOC GAC data, the number of observations available in any given 60-hour period will likely increase. The Navy would also have the opportunity to increase the number of retrievals in the 11 x 11 target array. This increase would permit more precise location of fronts and eddies in the objective analysis routines, since a 10-km, SST-only analysis currently under development at NORDA will be ready to accept the data.

VII. FNOC 40-km Gulf Stream regional EOTS runs without MCSSTs

The 63 x 63 version of the Gulf Stream regional EOTS analysis has been run since 1981 with approximately 40-km grid point resolution. The purpose of the tests described here is to determine the impact that satellite SSTs have on the final SST field generated by EOTS. This examination was accomplished by running two parallel versions of EOTS offline in which one had access to all observations (i.e., MCSSTs, ship/buoy, XBT, and bogus messages), but the other was denied the use of the MCSSTs. The following discussion first considers the test where satellite data were withheld.

The two EOTS runs were made daily at 12Z, 16–20 July 1985, using the data detailed in the previous section. Figure 13a is a contoured map of the SST field generated by EOTS on 16 July without access to the MCSSTs. This field is contoured at 1°C intervals and uses climatology as its initial condition. The Gulf Stream system is clearly evident, as well as the four or five warm core eddies and several cold core rings south of the stream. These prominent mesoscale features are retained in the field solely due to use of a satellite infrared bogus (Fig. 5) generated by Norfolk, as reported in an earlier section.

The EOTS run for 17 July (Fig. 13b) then uses the field derived for the 16th (not climatology) as its starting point. Since the bogus is only updated once a week on Thursday afternoon, each subsequent SST field should look more or less the same unless a wealth of new data becomes available. Without the MCSSTs, this assumption is typically true. Several hundred new ship/buoy reports are available, but their data density and own inaccuracies (ship RMS error = 1.5°C) do not allow them to significantly impact the analysis.

The large scatter associated with ship reports can be seen in any of the EOTS runs without satellite SSTs. Figures 13a–e are relatively noisy in the Sargasso Sea and contain several suspect areas on the far eastern boundary. The bull's-eye like pattern is indicative of one or two ship engine intake readings that do not truly reflect the ambient SST values. EOTS has several methods to filter out bad SSTs, but apparently a few questionable ship observations slipped through the quality control routines. The five SST analyses also exhibit a rather smoothed shelf-slope front near 42°N. This front is typically quite sharp and can often have a 4–5°C gradient occurring well within two 40-km grid points.

The 20 July 1985 EOTS run without MCSSTs does show a change directly related to the weekly input of an updated fronts and eddies bogus message. The warm rings have been modified slightly, but the two cold rings are much more pronounced after assimilating the new data. There is also a reorientation where the Gulf Stream north wall meanders near 62°W. These alterations would have been more noticeable if a new ring had formed and been included in the bogus update.

VIII. FNOC 40-km Gulf Stream regional EOTS runs with MCSSTs

The identical 63 x 63 40-km resolution EOTS program was rerun while including the MCSSTs. Figures 14a–e are the resulting EOTS SST fields for 16–20 July 1985. The 16 July field (Fig. 14a) immediately reveals several differences when compared to the version without the incorporation of satellite data (Fig. 13a). The SST field with MCSSTs is less noisy in the Sargasso Sea and tends to emphasize the meridional gradient.

Figure 14a also illustrates a rearrangement of the shelf-slope front near 41°N to 42°N and the temperature field around Nova Scotia. It is interesting that these changes have occurred with only one iteration through EOTS. Both runs started with the same climatology, but the inclusion of the satellite infrared data has already significantly affected the fields. Most of the bull's-eye type features on the far eastern section of Figure 13a are not present in Figure 14a and indicate that there were enough accurate MCSSTs to compensate for the ship data causing these problems.

The series of EOTS SST fields that assimilate MCSSTs increasingly sharpen the shelf-slope front. Thus, the available data is adequate to tighten the smooth climatological pattern used as an initial condition and to more realistically represent the existing gradient. After four days, the SST field (Fig. 14d) has a well defined shelf-slope front, five warm core rings that stand out from the surrounding slope water and a well-defined

north wall. The cold rings have lost some of their infrared signature, but this loss is reinforced when the new bogus goes into effect on the 20th (Fig. 14e). Figure 14e does have some noise in the field south of the Gulf Stream, but it is significantly better than the version generated without the use of MCSSTs.

IX. Difference fields between EOTS SST fields with/without MCSSTs (40 km)

Difference fields were generated to be able to delineate those areas of disagreement between the SST fields produced with and without MCSST data. One can visually spot the major areas of conflict when viewing the two patterns side by side, but some of the more subtle discrepancies would not be seen without this type of plot. Figures 15a–e illustrate the fact that the differences grow in magnitude and areal coverage with time. Figure 15a reveals that the 16 July SST fields differ in several ways: the bull's-eyes produced by the ship data are quite apparent, the MCSST version is 0.5°C warmer southeast of Long Island, and two broad areas of small changes occur along the axis of the Gulf Stream.

These three characteristics are enhanced in Figure 15b, which compares the two fields on the next day (17 July). The magnitude of the previous differences has increased such that 1.5°C anomalies now result. These zones of conflict are also joined by a large area of disagreement along the shelf-slope front, as noted earlier, and by a complex region of mismatches in the Sargasso Sea.

These last two areas of difference continue to amplify with time to the point that they dominate the fields. Note that the relative weighting of XBT, MCSST, and ship/buoy data used in this study was exactly that used in the operational EOTS runs. Thus, the study proves that MCSST data is strongly impacting the FNOC regional EOTS products.

X. FNOC 125 x 125 20-km Gulf Stream regional EOTS runs without MCSSTs

The 40-km regional EOTS analysis for the Gulf Stream can map out many of the mesoscale ocean features. However, as mentioned previously, higher grid resolution is needed to adequately handle the many fast-evolving small rings and meanders associated with this current system. Therefore, in 1985 FNOC implemented an operational 20-km EOTS Gulf Stream analysis that uses a 125 x 125 grid array instead of the standard 63 x 63 version. This section details an offline test of this analysis, again investigating the impact of MCSSTs. It also provides an excellent chance to compare the mapping capabilities of the two resolutions.

The first 20-km run without the use of MCSST data clearly reveals some of the advantages and disadvantages of mapping with higher resolution grids (Fig. 16a). The north and south wall of the Gulf Stream are considerably sharper, as is the definition of the warm and cold core rings, and is much more realistic than that detailed in the 40-km version. However, the 20-km grid can also enhance bad portions of the data base more graphically than the 40-km analysis. This is the case on the extreme eastern side of the domain near 28–32°N. Several apparently poor ship observations have caused the 20-km analysis to draw bull's-eyes that are more pronounced than those in the previous 40-km version. This points out the fact that quality control should not only be a major issue, but must become even stricter when the resolution of the analysis increases.

The 20-km EOTS runs without MCSST data (Figs. 16a–e) display some of the same noise problems inherent in the 40-km maps. The Sargasso Sea is depicted by jumbled contours that get progressively more confusing as the analysis cycles on itself. By the fifth day (Fig. 16e), the Sargasso Sea is just one big mess of closed contours, and it is difficult to pick out the overriding SST pattern. This morass is in direct contrast to the well-defined region of the slope water, where a fresh bogus has located the rings and stream quite well and the shelf-slope front is discernible.

XI. FNOC 125 x 125 20-km EOTS runs with MCSST data

The tests with satellite data in the 40-km analysis exhibited two main trends: the shelf-slope front was enhanced considerably, and the noise in the Sargasso Sea produced by ship observations was reduced significantly. These positive attributes of MCSST data are evident again in even greater magnitude in the 20-km analyses. Figure 17a begins by showing how the MCSST data (Fig. 12a) in the eastern portion of the grid has eliminated several of the disturbing bull's-eyes attributed to poor ship observations (Fig. 16a). The one remaining bull's-eye slowly fades as additional information corrects it during the five-day period.

Figure 17e indicates that a certain amount of noise is still present in the Sargasso Sea (as shown by the variety of closed contour features), but the dominant meridional pattern comes through with 28, 27, and 26°C contours stretching across the width of the region. This same figure also depicts the shelf-slope front well, but could still use some additional packing of the isotherms. More MCSSTs would probably map this large temperature gradient better.

The MCSST data also appears to have a positive impact on the mapping of the warm core rings north of the stream. Figures 17a–e indicate that the MCSSTs do enhance the field such that the gradients of the rings are not spread outward,

and the tight gradients are retained on the boundary. The rings are also seen to be separated from the shelf-slope front by a zone of slope water that is relatively homogeneous.

The effect of going from a 40-km to a 20-km grid should be emphasized from the standpoint that strong mesoscale fronts and eddies are mapped much more precisely in the 20-km version. This factor is critical when using the EOTS products for a variety of ASW or Optimum Track Ship Routing (OTSR) missions.

XII. Difference fields between EOTS runs with/without MCSSTS (20 km)

Figures 18a–e display the differences between the 20-km EOTS runs with/without the incorporation of satellite SST data. The general pattern of these fields is quite similar to the previous ones using the 40-km data, but the higher resolution tends to magnify some of the differences. We have adjusted the contour interval in Figure 18 to 1°C, compared to 0.5°C for Figure 15. This adjustment was necessary in order to observe the large values in several regions.

Differences in the two analyses reach 3–4°C by 18 July (Fig. 18c) along the shelf-slope front, indicating that there are enough MCSSTs to adjust the position and magnitude of this sharp feature. This variation is to be expected, since the shelf-slope front is the next largest high-gradient area after the north wall of the Gulf Stream. Since both analyses use the same bogus message to define the north wall, mapping of its boundary is typically better than the shelf-slope front. The inclusion of MCSSTs thus has little impact on the north wall because of the inherent way the bogus data is incorporated. The bogus is dominant and overrides all other data sources.

XIII. Effect of MCSSTs on subsurface thermal structure

The FIB technique incorporated within EOTS utilizes a vertical blending process that translates surface thermal information into subsurface thermal data. This process works reasonably well in regions of SST fronts produced by strong dynamical ocean features (e.g., western boundary currents, new warm and cold core rings), since these fronts correlate fairly well with the temperature structure below. Each case may have a slightly different tilt to the frontal region with depth, but for mapping on a 20-km or 40-km grid, the assumptions contained within EOTS do a reasonable job.

Therefore, one question to be explored is whether or not the addition of MCSST data significantly affects the way EOTS maps the subsurface thermal field. The preliminary answer would appear to be yes, since the SST patterns generated with/without MCSST data are obviously not identical. To verify this assumption, we have produced temperature maps for the EOTS level at 50 m using the 63 x 63 40-km Gulf Stream analysis.

Figure 19a is the 50-m EOTS temperature field generated without the use of MCSST data for 16 July. The pattern is as smooth as expected, since the first guess was climatology and the number of XBTs available to modify the thermal structure directly is not significant. The north and south wall of the Gulf Stream are evident, as well as the warm and cold core rings seen earlier in the SST maps. The 50-m fields for 17–20 July indicate that the Sargasso Sea contains somewhat more noise by day 5 and that the eastern boundary differences (bull's-eyes) also propagate downward. On the favorable side, the slight tightening of the shelf-slope seen on the corresponding SST maps appears here as well and indicates that the product is improving progressively as the analysis cycles daily.

The 50-m temperature fields (Figs. 20a–e) that utilize MCSST data exhibit many of the same characteristics of the SST maps. The noise in the Sargasso Sea is less, the warm core eddies are nicely embedded in slope water (retaining their gradients), and the shelf-slope front has been sharpened considerably. Thus, at first glance, the inclusion of MCSST data appears to correct the 50-m subsurface field in the direction required to more closely match the true ocean temperature structure as we understand it today.

We also produced difference maps similar to those presented earlier, where the 50-m temperature field from the analysis without MCSST data is subtracted from the corresponding field from the analysis with MCSST data. Figures 21a–e have many of the same characteristics noted in the SST difference maps. The bull's-eyes on the far eastern section, minor disagreements in the Sargasso Sea due to noise in the ship observations, and discrepancies along the shelf-slope front are similar to the earlier findings. The only readily detectable change is the smaller order of magnitude associated with the temperature differences, since the EOTS vertical blending technique results in subsurface anomalies whose amplitudes decay with depth.

XIV. Summary and conclusions

This report has clearly defined the importance of the Gulf Stream fronts and eddies bogus derived from IR imagery. EOTS 20-km analyses, which have access to all available XBTs, ships/buoys, MCSSTs, but not the bogus, cannot adequately map the mesoscale features of interest. The high quality and quantity of MCSST data is not sufficient by itself, when utilizing the FIB blending technique.

MCSST data produces significant changes in the SST field in the Gulf Stream regional EOTS analyses relative to EOTS runs without this data. These changes are consistent with our understanding of the oceans' thermal fields and indicate that the quality of the MCSSTs is quite high. The use of MCSSTs with accuracies near 0.6°C has smoothed out areas where noisy

ship observations once dominated in the Sargasso Sea. The SST gradients around the warm core rings have been retained, the shelf-slope front has been realigned and tightened considerably, and the overall field appears enhanced when the satellite infrared reports are included.

We have also seen how higher resolution analyses (20 km versus 40 km) have been able to more accurately depict the many abrupt ocean thermal features that are present in the Gulf Stream region. This benefit was especially true for the shelf-slope front. This development bodes well for totally automated objective analysis efforts. The Navy would like to work toward the day when bogus messages are not required. An expanded data base of MCSSTs and passive-microwave-derived SSTs may allow us to map the tactical mesoscale fronts and eddies on several different spatial scales without human manipulation.

The MCSST data also has the capability to modify the subsurface thermal field by using the vertical blending process in EOTS. This process helps in many strong frontal zones where the SST field is well known and correlates well with subsurface features. This vertical blending is not necessarily desirable in regions with shallow features. We still lack sufficient subsurface in situ data to do the job desired. This is an area where altimetry holds promise in providing additional data directly related to parameters such as the depth of the thermocline. Replacement of the FIB-based EOTS by an optimal estimation technique will also help. OTIS (Innis, 1985) will provide a basis for rationally assimilating all the available data based on the known statistics of the ocean. When combined with altimetry, OTIS will extend the usefulness of available XBTs below the seasonal thermocline. When combined with regional TOPS models, OTIS will help provide the variability due to synoptic scale forcing above the seasonal thermocline.

XV. References

Bernstein, R. L. (1982). Sea Surface Temperature Estimation Using the NOAA 6 Satellite Advanced Very High Resolution Radiometer. *Journal of Geophysical Research*, v. 87, n. C12, pp. 9455–9465.

Bernstein, R. L. and D. B. Chelton (1985). Large-Scale Sea Surface Temperature Variability from Satellite and Shipboard Measurements. *Journal of Geophysical Research*, v. 90, c. 6, pp. 11,619–11,630.

Bowers, D. G., P. J. E. Crock, and J. H. Simpson (1982). An Evaluation of Sea Surface Temperature Estimates from the AVHRR. *Conference on Remote Sensing and the Atmosphere*, Liverpool, England, 15–17 December.

Brower, R. L., H. S. Gohrband, W. G. Pichel, T. L. Signore, and C. C. Walton (1976). *Satellite Derived Sea Surface Temperature from NOAA Spacecraft*. NOAA Tech Memo NESS 78, Dept. of Commerce, Washington, D.C., p. 74.

Clancy, R. M. and K. D. Pollack (1983). A Real-Time Synoptic Ocean Thermal Analysis/Forecast System. *Progress in Oceanography*, v. 12, pp. 383–424.

Gandin, L. S. (1965). Objective Analysis of Meteorological Fields. *Israel Program for Scientific Translations*, Jerusalem, p. 242.

Hilland, J. E., D. B. Chelton, and E. G. Njoku (1985). Production of Global Sea Surface Temperature Fields for the Jet Propulsion Laboratory Workshop Comparisons. *Journal of Geophysical Research*, v. 90, c. 6, pp. 11,642–11,650.

Holyer, R. J. and J. D. Hawkins (1982). *Comparison of Multichannel and Two-Satellite Methods for Remote Measurement of Sea Surface Temperature*. Naval Ocean Research and Development Activity, NSTL, Mississippi, NORDA Technical Note 162, 9 pp.

Holl, M. M., M. J. Cuming, and B. R. Mendenhall (1979). *The Expanded Ocean Thermal Structure Analysis System: A Development Based On the Fields-By-Information Blending Methodology*. Technical Report M-241, Meteorology International Inc., 2600 Garden Road, Suite 145, Monterey, California 93949.

Innis, G. E. (1983). *Progress In Implementing the Optimum Thermal Interpolation System (OTIS) at FNOC*. Technical Report SAI-085-83-429-LJ, Science Application International Corporation, 1200 Prospect Street, P.O. Box 2351, La Jolla, California 92038.

Innis, G. E. (1985). *Further Development and Implementation of the Optimum Thermal Interpolation System (OTIS) at FNOC*. Technical Report SAI-85-1635, Science Applications International Corporation, 1200 Prospect Street, P.O. Box 2351, La Jolla, California 92038.

McClain, E. P. (1980). Multiple Atmospheric Window Techniques For Satellite Derived Sea Surface Temperatures. *COSPAR Symposium on Oceanography from Space*.

McClain, E. P. (1980). Results of Global Tests of a Two-Window Method For Satellite Derived Sea Surface Temperature. *Workshop on Application of Existing Satellite Data to the Study of Ocean Surface Energetics*, 19–21 November.

McClain, E. P. (1981). Split-Window and Triple-Window Sea Surface Temperature Determinations from Satellite Measurements. *1981 ICES Statutory Meeting*, 6–10 October.

McClain, E. P. (1981). Multispectral Approaches to Satellite-Derived Sea Surface Temperatures. *AGU Spring Meeting*, Baltimore, Maryland, 25–29 May.

McClain, E. P., W. G. Pichel, C. C. Walton, A. Ahmad, and J. Sutton (1982). Multi-Channel Improvements to Satellite-Derived Global Sea Surface Temperatures. *Proceedings of XXIV COSPAR Symposium*, 22–29 May.

McClain, E. P., W. G. Pichel, and C. C. Walton (1985). Comparative Performance of AVHRR-Based Multichannel Sea Surface Temperatures. *Journal of Geophysical Research*, v. 90, c. 6, pp. 11,587–11,601.

McClain, E. P. (1986). *Minutes of the 53rd Meeting of the Sea Surface Temperature Research Panel (SSTRP).* NESDIS, Washington, D.C., 3 March.

Pichel, W. G., Personal communication.

Rao, R. K., W. L. Smith, and R. Koffler (1972). Global Sea-Surface Temperature Distribution Determined fron an Environmental Satellite. *Monthly Weather Review*, v. 100, c. 1, pp. 10–14.

Shenk, W. E. and V. V. Solamonson (1972). A Multispectral Technique to Determine Sea Surface Temperature Using Nimbus-2 Data. *Journal of Physical Oceanography*, v. 2, pp. 157–167.

Smith, W. L., P. K. Rao, R. Koffler, and W. R. Curtis (1970). The Determination of Sea Surface Temperature from Satellite High Resolution Infrared Window Measurements. *Monthly Weather Review*, v. 98, pp. 604–611.

Strong, A. E. and E. P. McClain (1985). Improved Ocean Surface Temperatures from Space-Comparison with Drifting Buoys. *Bulletin of the American Meteorological Society*, v. 65, pp. 138–142.

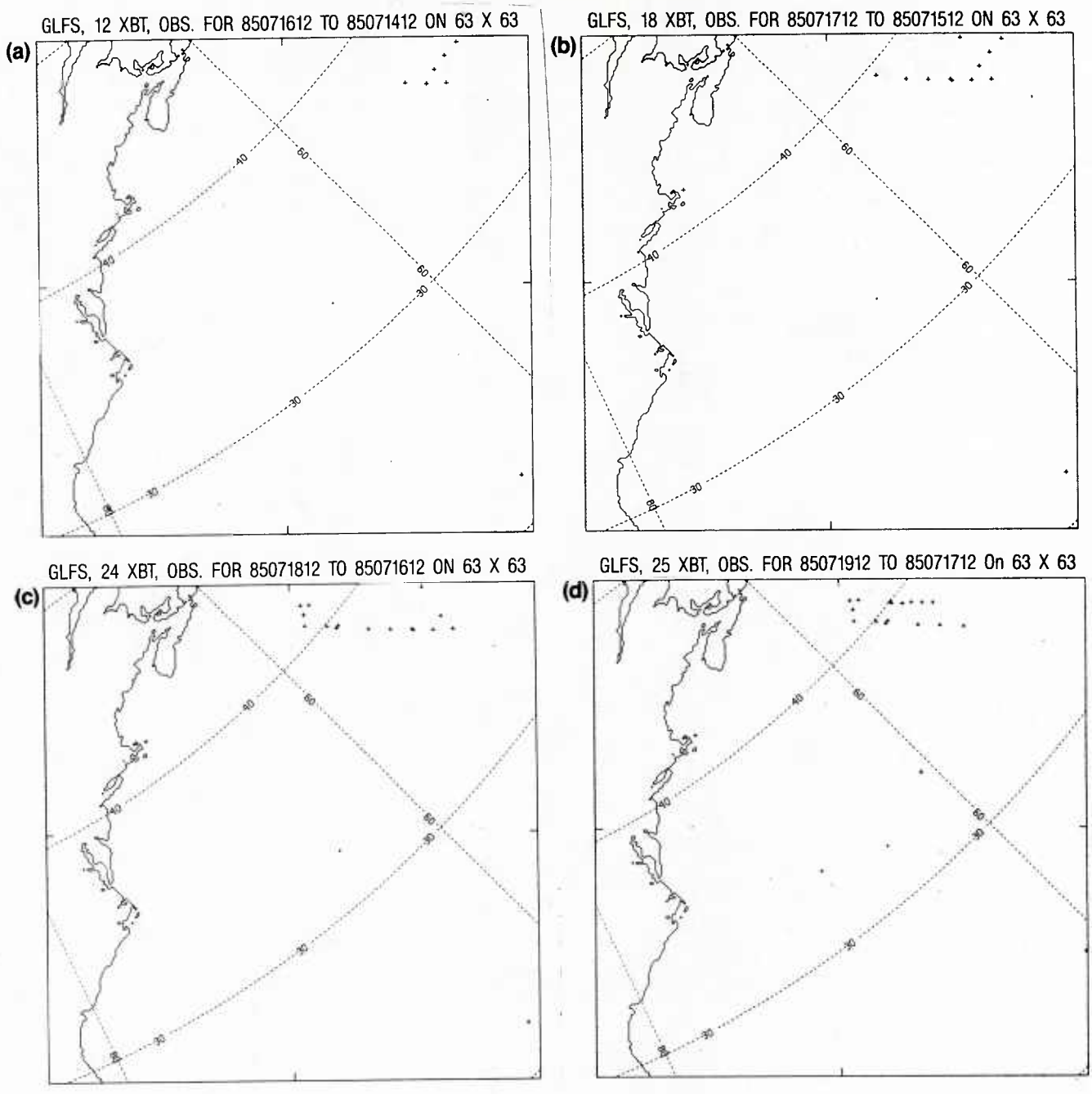

Figure 10. (a, b, c, d) Data distribution of XBTs for the 48-hour period ending at 12Z on 16, 17, 18, and 19 July 1985.

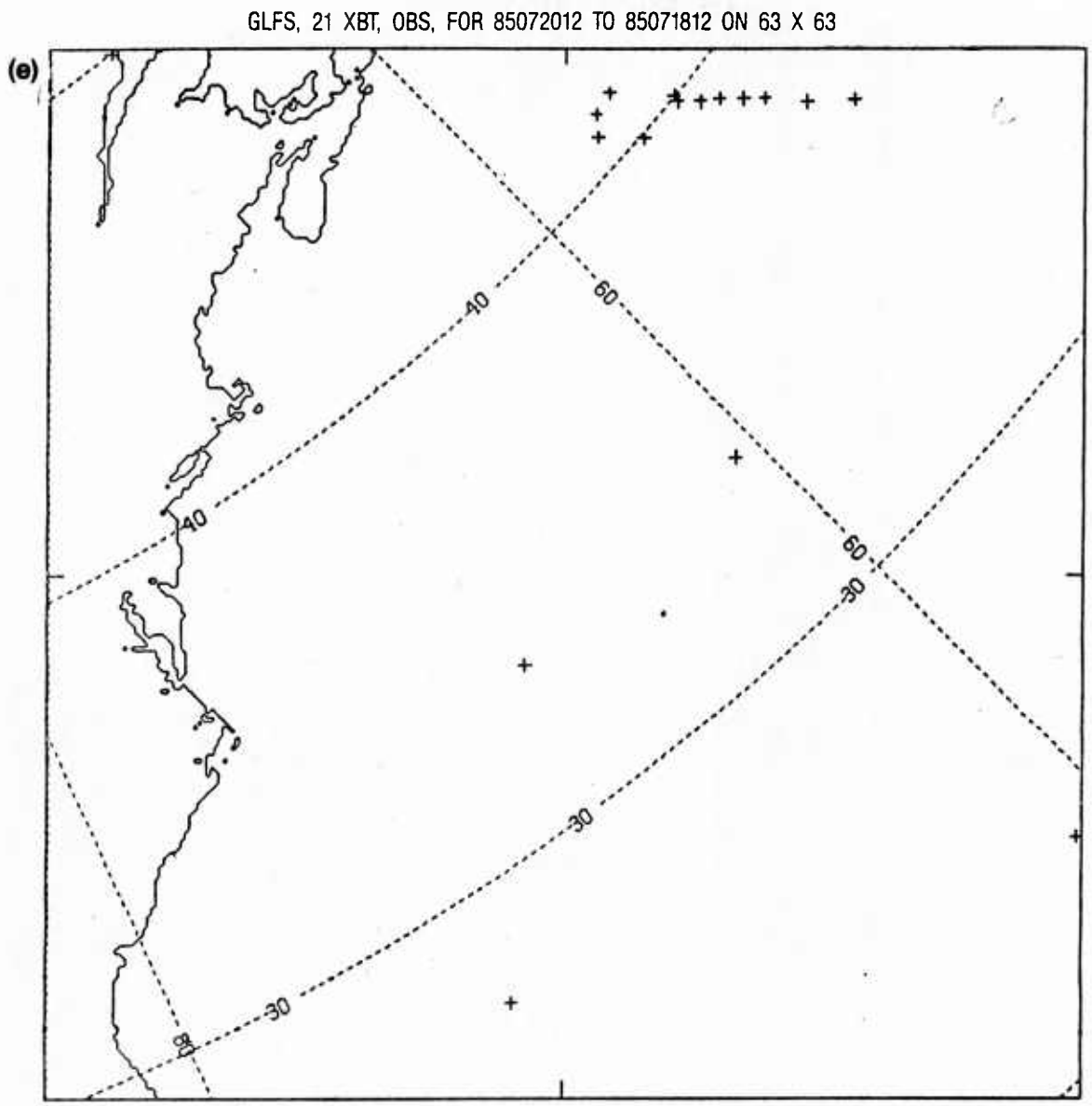

Figure 10. (e) Data distribution of XBTs for the 48-hour period ending at 12 Z on 20 July 1985.

GLFS REGION, SHIP LOCATIONS

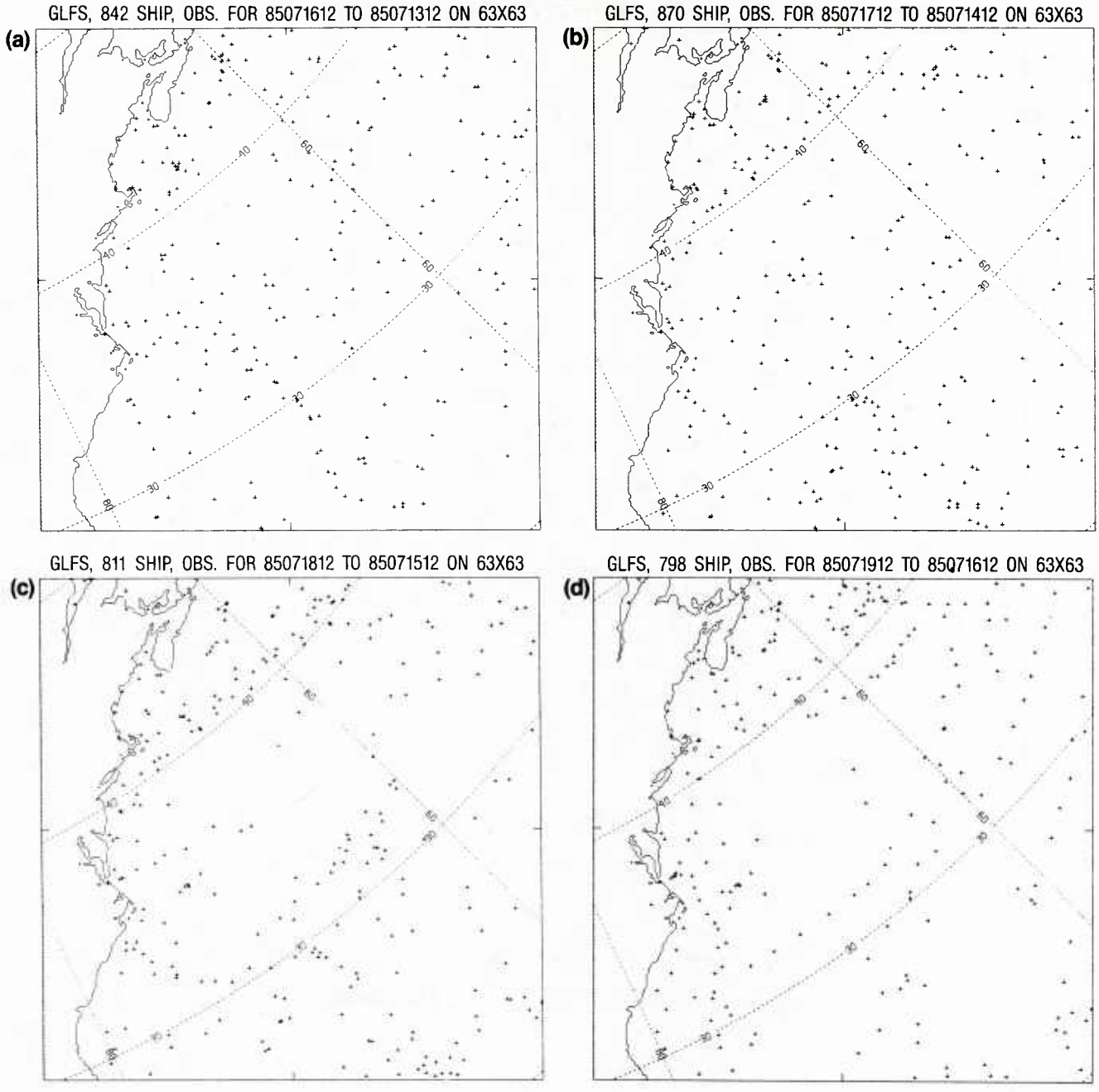

Figure 11. (a, b, c, d) Data distribution of ship/buoy reports over latest 72 hours starting at 12Z on 16, 17, 18, and 19 July 1985.

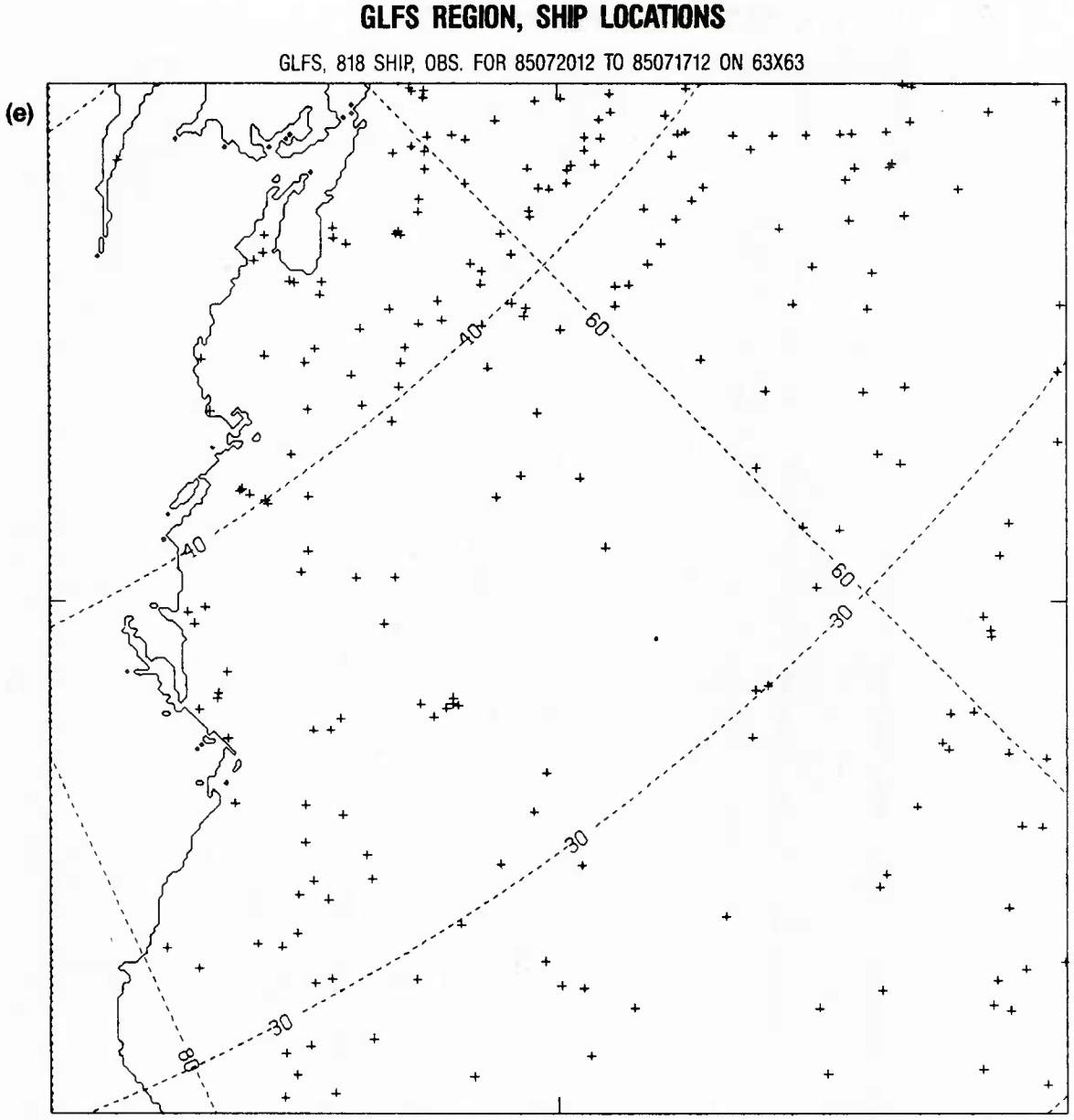

Figure 11. (e) Data distribution of ship/buoys reports over latest 72 hours starting at 12Z on 20 July 1985.

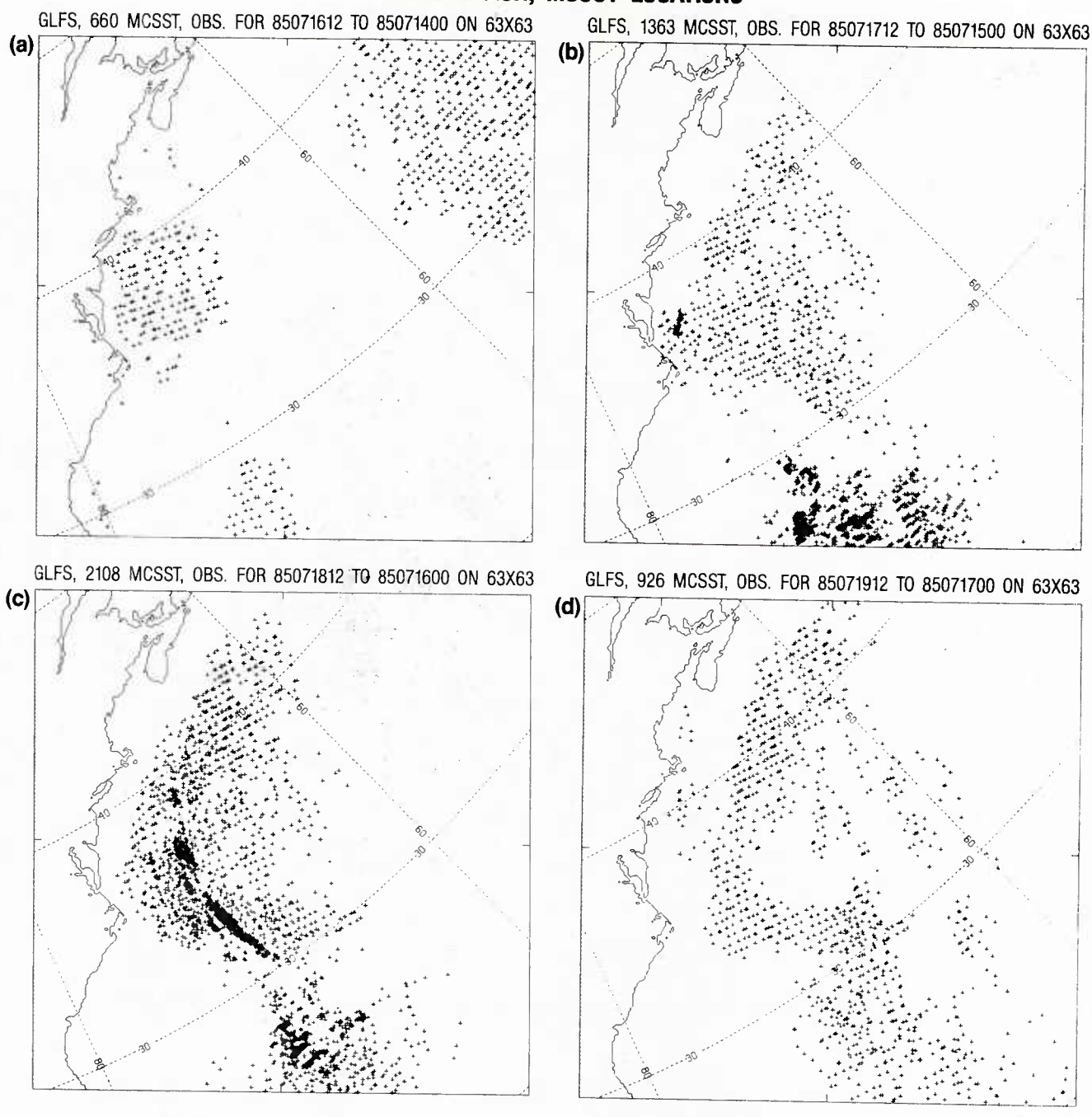

Figure 12. (a, b, c, d) Data distribution of MCSSTs for the last 60 hours starting at 12Z on 16, 17, 18, and 19 July 1985.

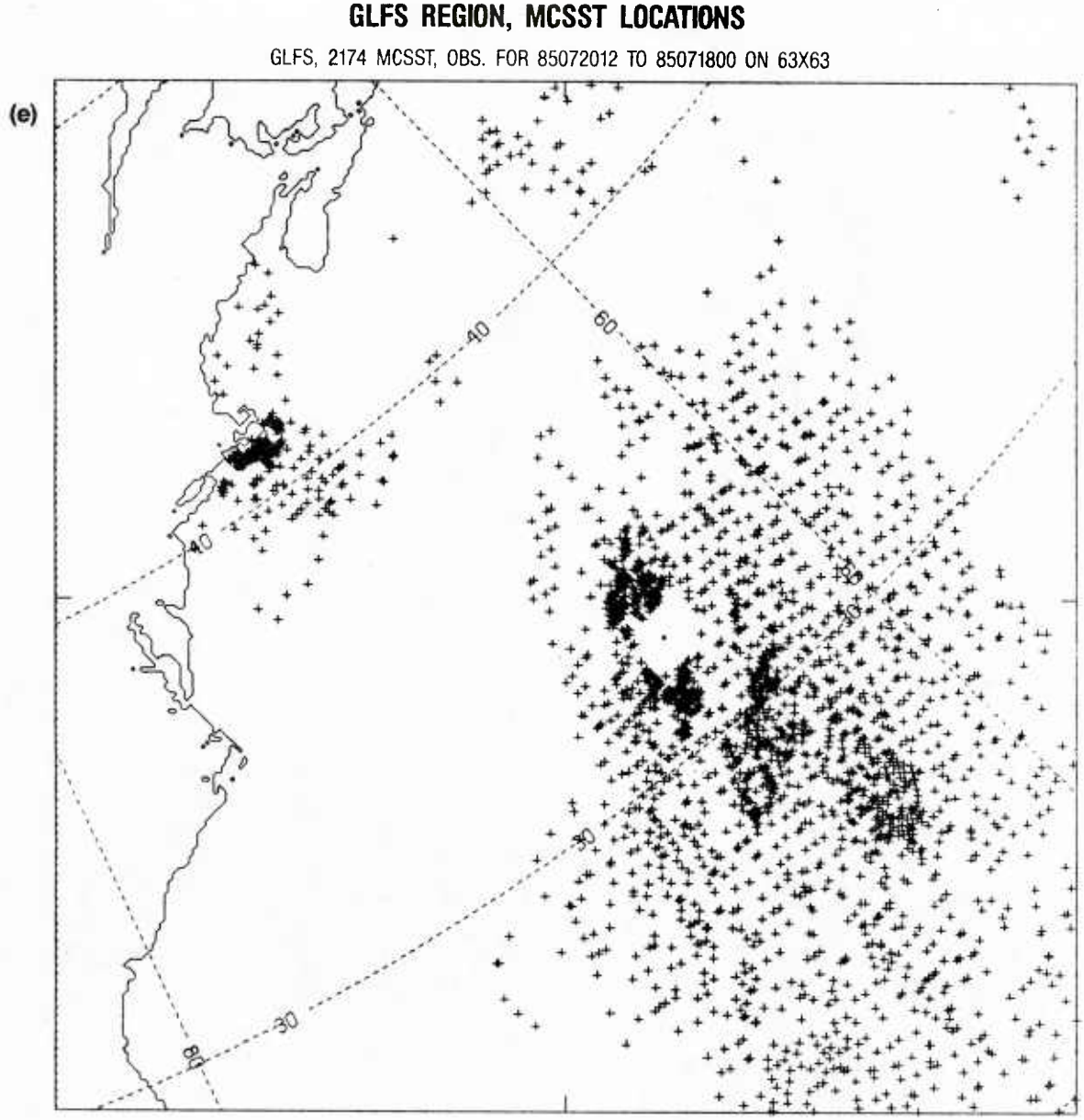

Figure 12. (e) Data distribution of MCSSTs for the last 60 hours starting at 12Z on 20 July 1985.

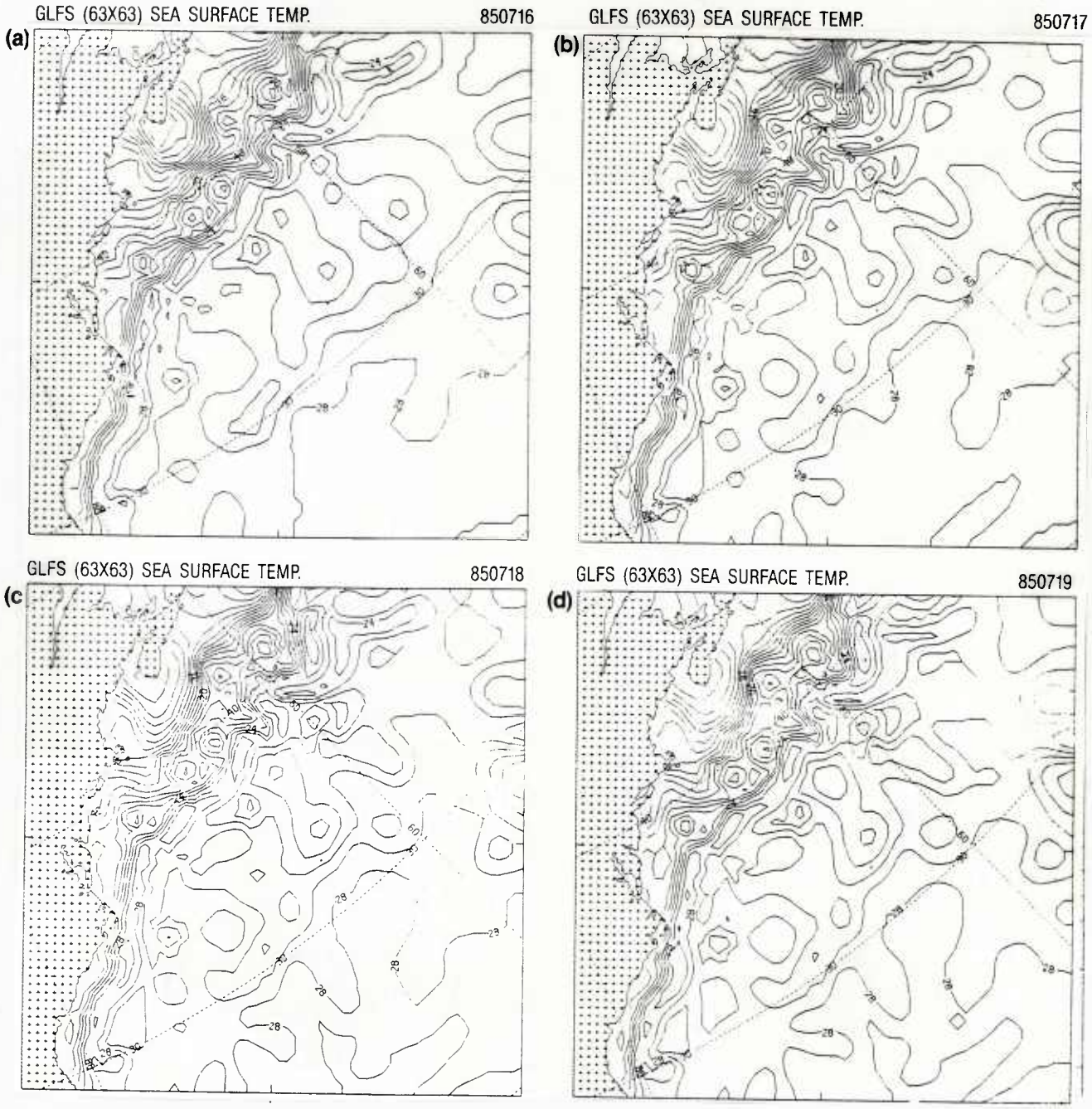

Figure 13. (a, b, c, d) EOTS Gulf Stream 40 km SST fields for 16, 17, 18, and 19 July 1985 without input of MCSST data.

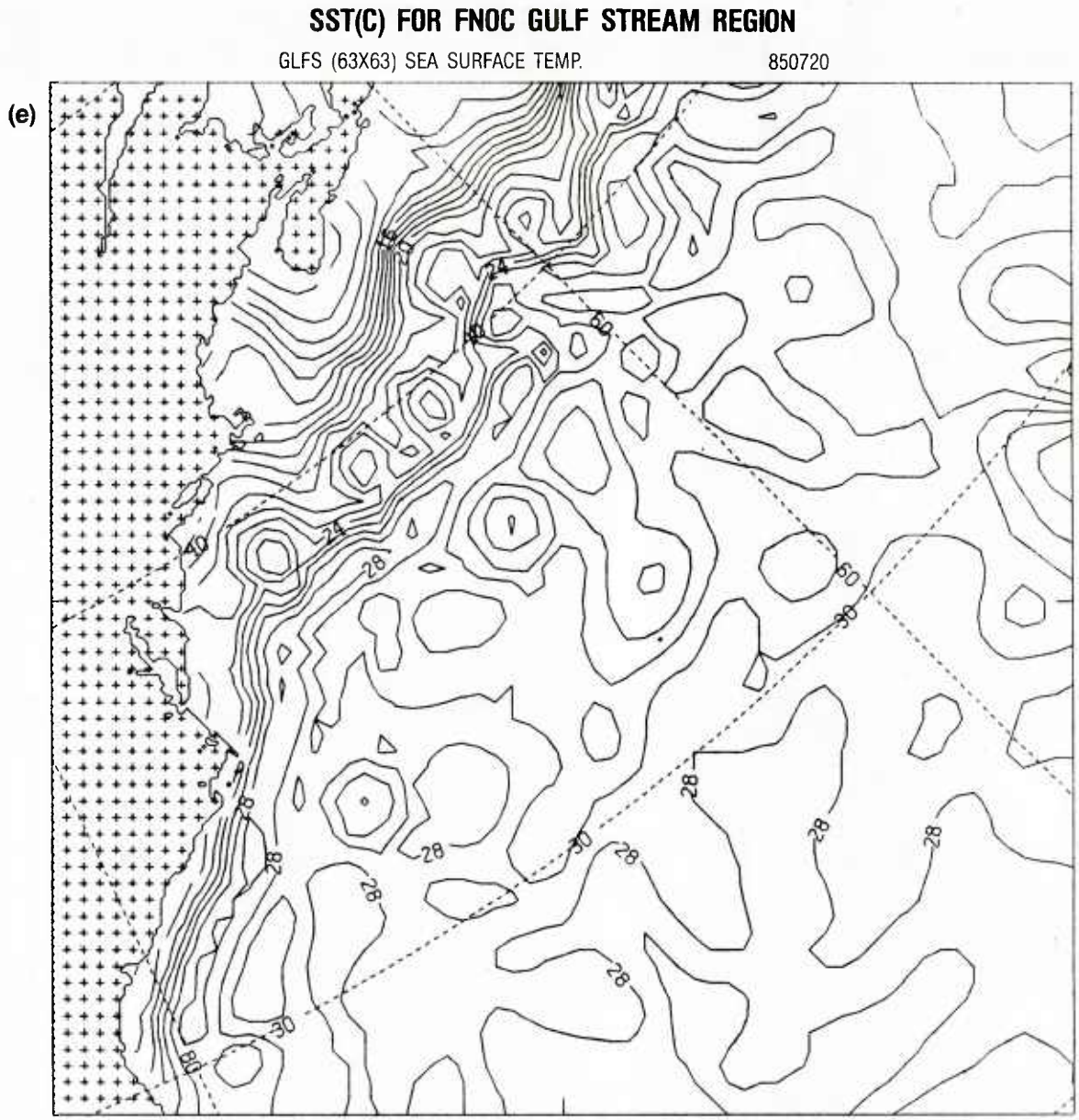

Figure 13. (e) EOTS Gulf Stream 40 km SST field for 20 July 1985 without input of MCSST data.

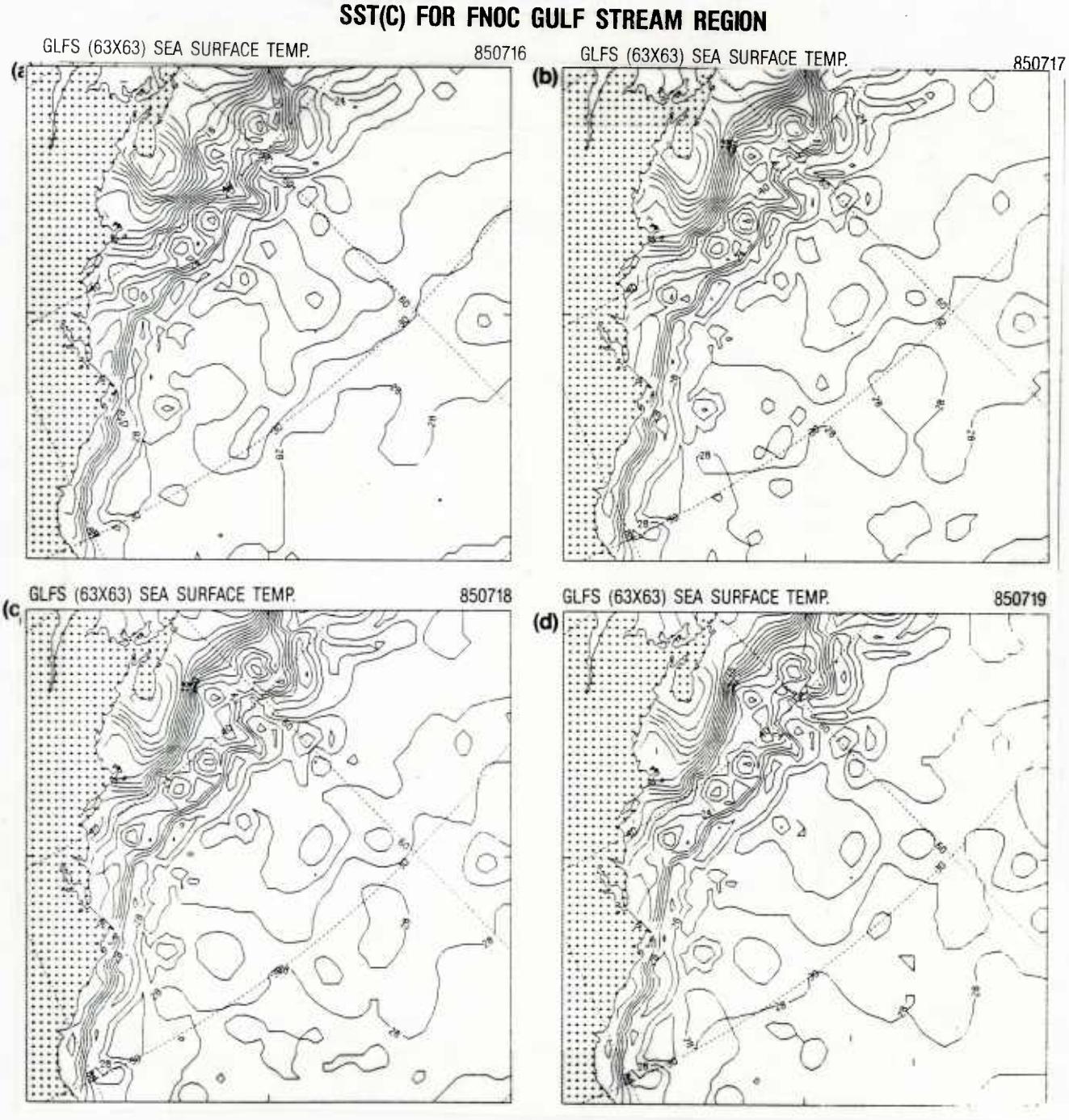

Figure 14. (a, b, c, d) EOTS Gulf Stream 40 km SST fields for 16, 17, 18, and 19 July 1985 incorporating 60 hours of MCSST data.

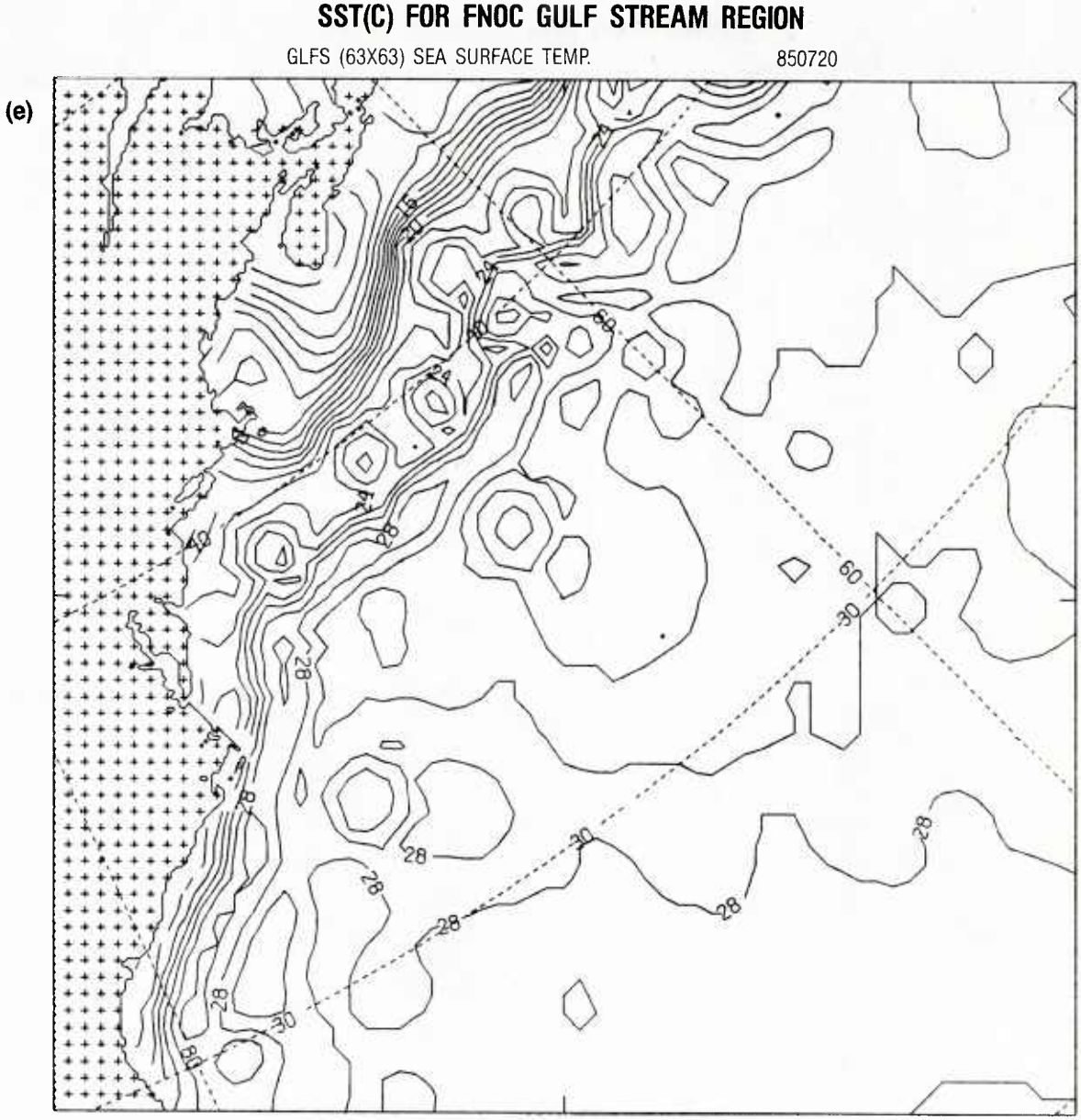

Figure 14. (e) EOTS Gulf Stream 40 km SST field for 20 July 1985 incorporating 60 hours of MCSST data.

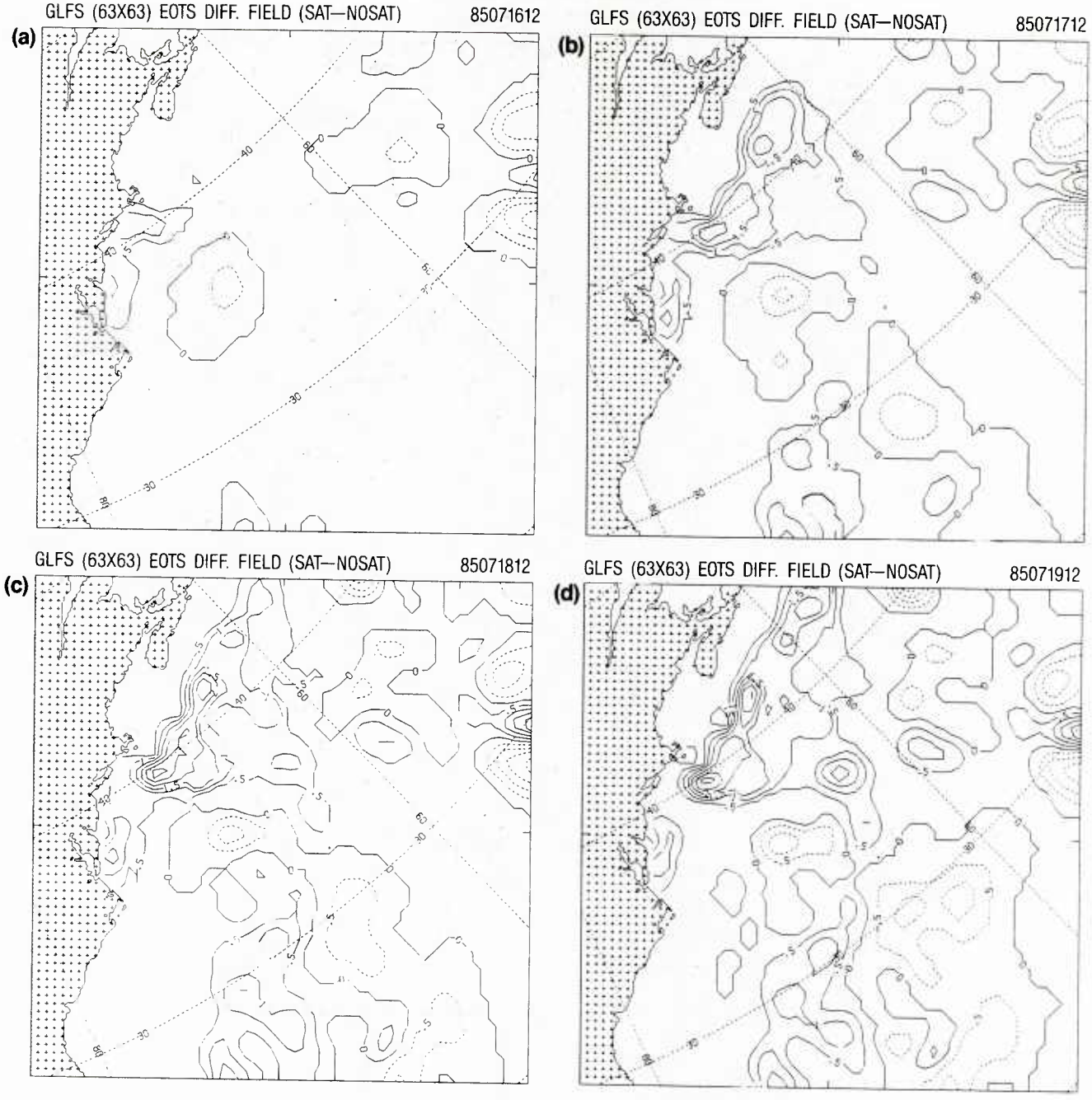

Figure 15. (a, b, c, d) Difference fields on 16, 17, 18, and 19 July 1985 for EOTS runs subtracting the SST field generated without MCSST from the one with MCSST data input.

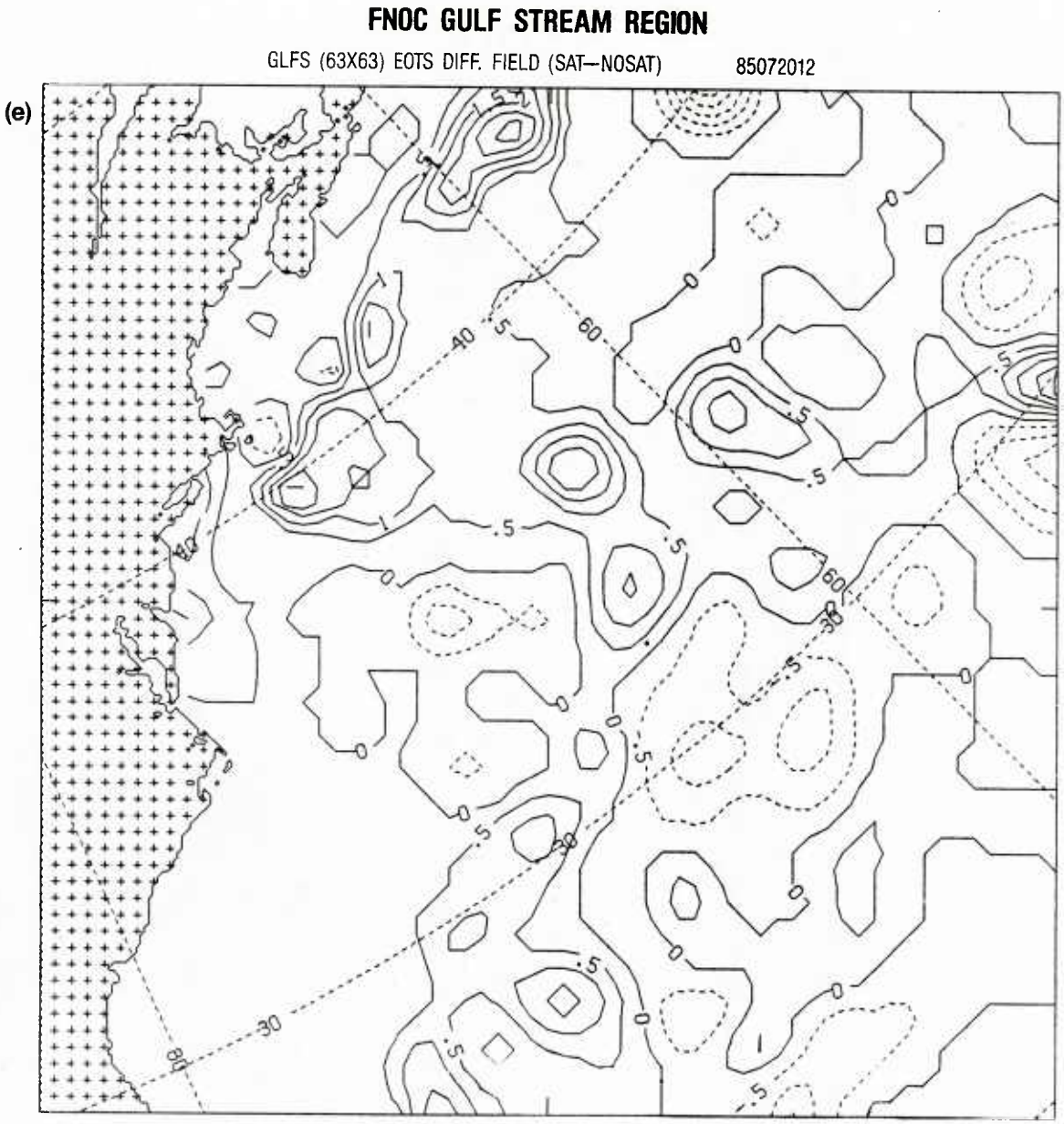

Figure 15. (e) Difference field between EOTS runs with/without MCSST data for 20 July 1985.

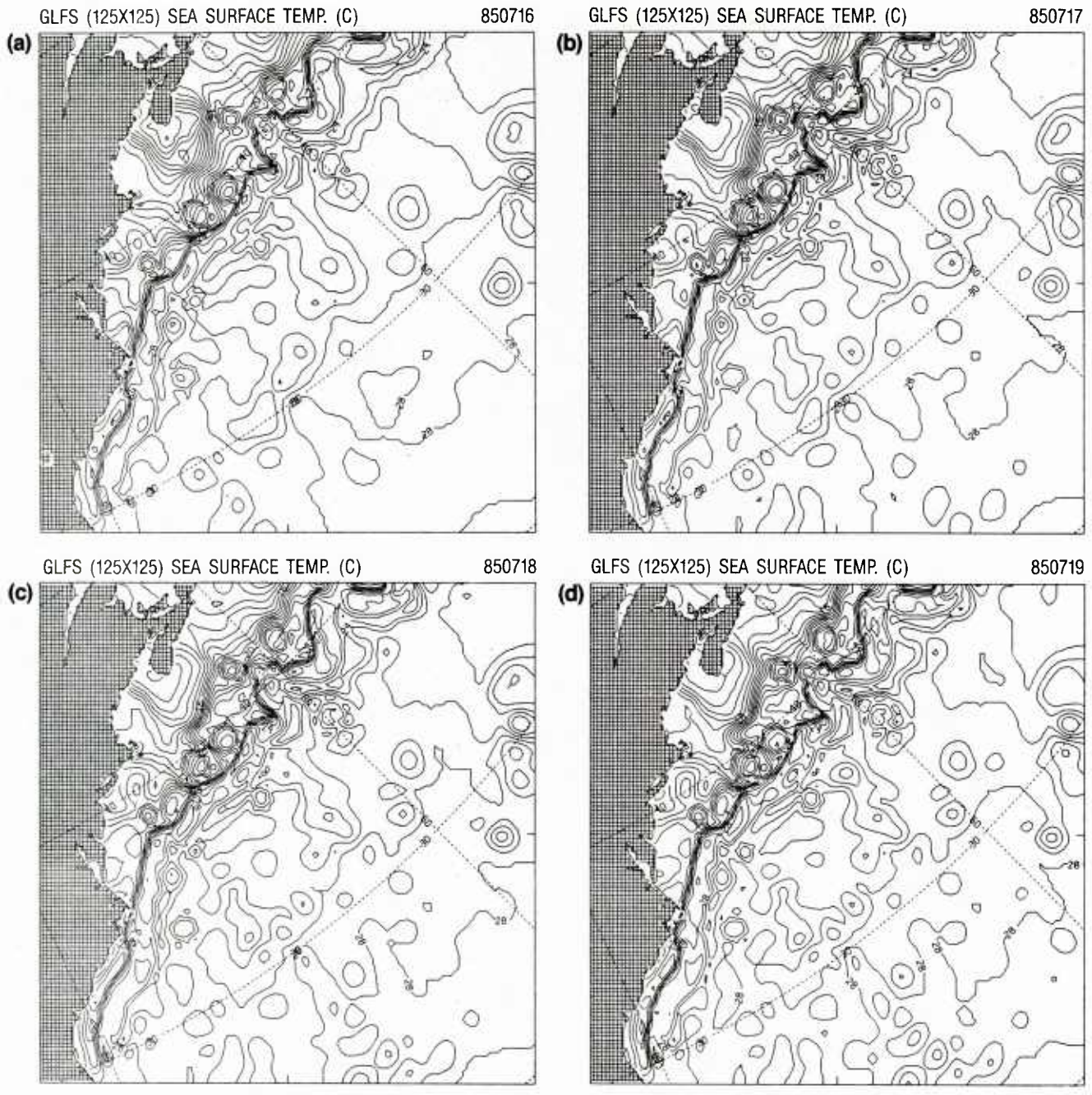

Figure 16. (a, b, c, d) The 20-km Gulf Stream regional EOTS SST field (1 °C contour) without MCSST data for 12Z 16, 17, 18, and 19 July 1985.

(e)

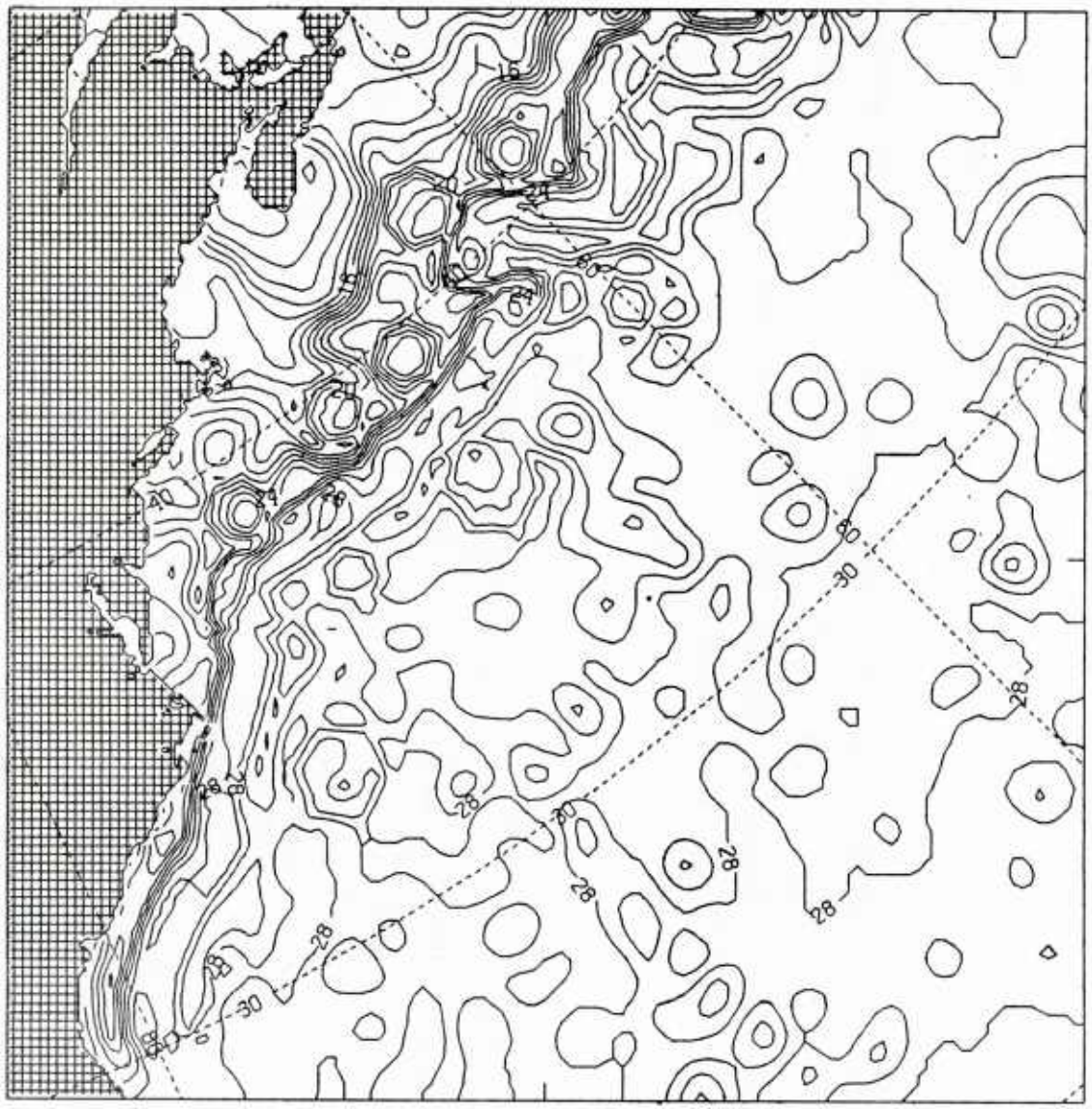

Figure 16. (e) The 20-km Gulf Stream regional EOTS SST field (1 °C contour) without MCSST data for 12Z 20 July 1985.

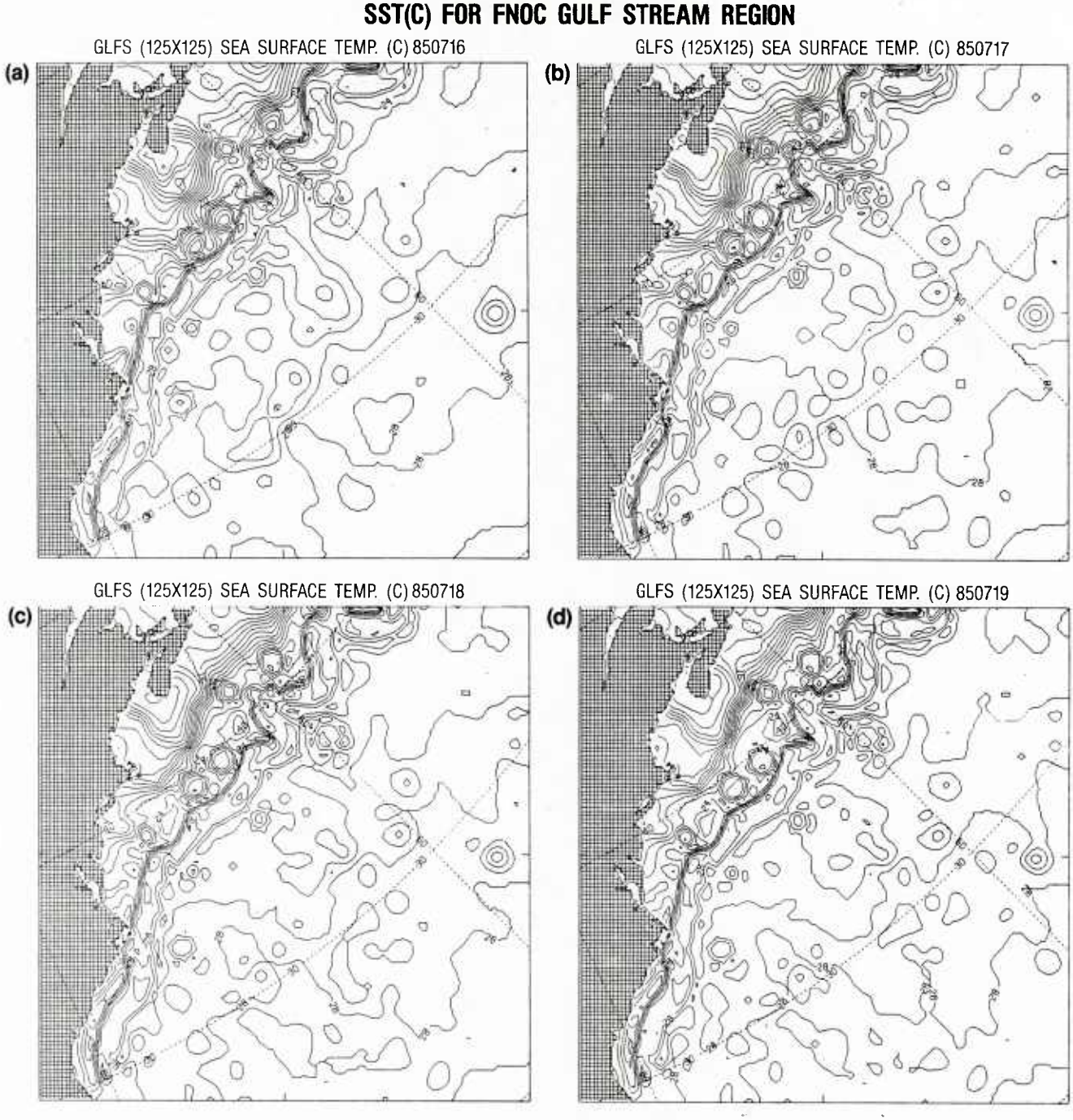

Figure 17. (a, b, c, d) The 20-km EOTS SST fields for 12Z 16, 17, 18, and 19 July 1985 that include the use of MCSST data.

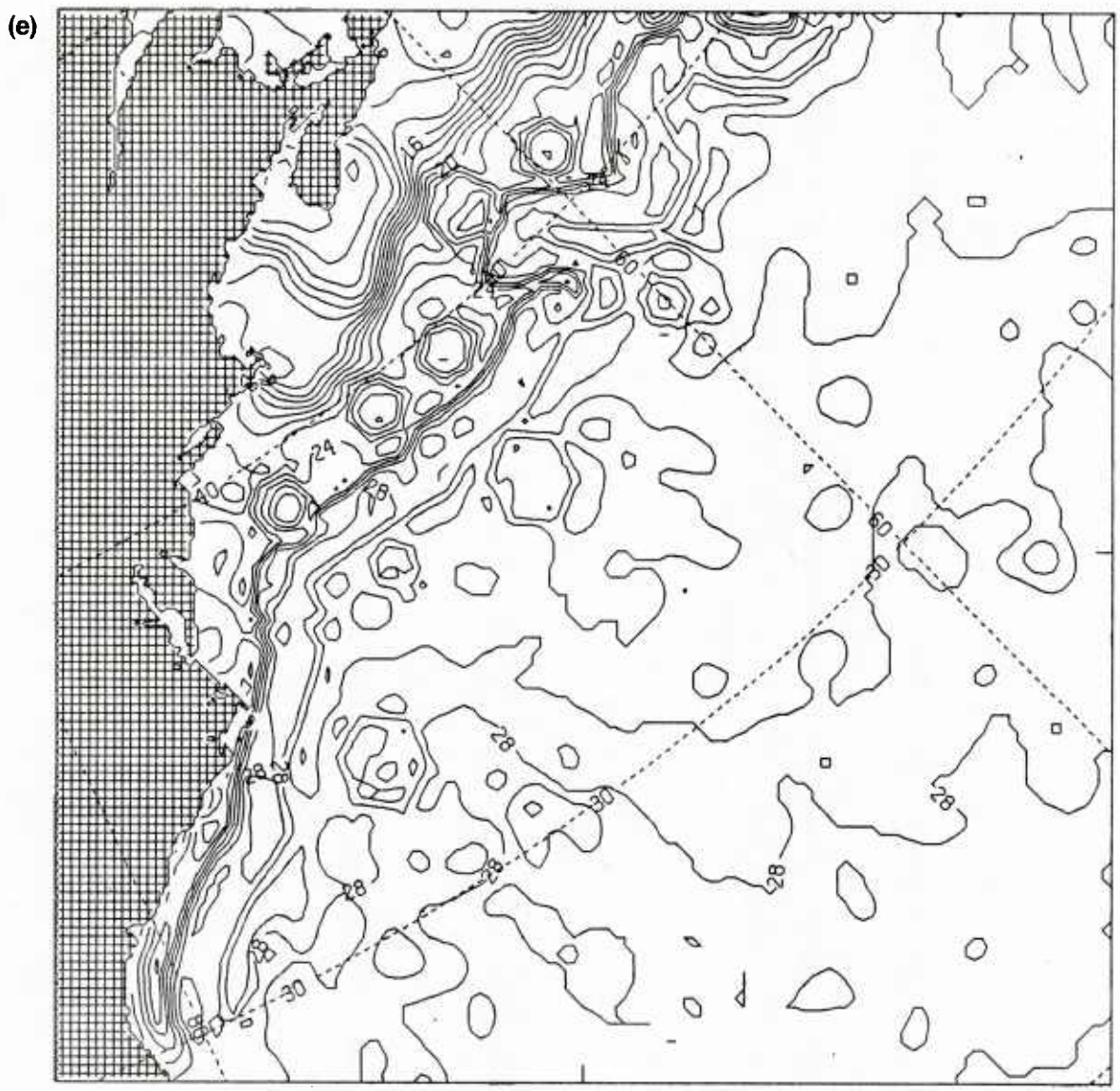

Figure 17. (e) The 20-km EOTS SST field for 12Z 20 July 1985 that includes the use of MCSST data.

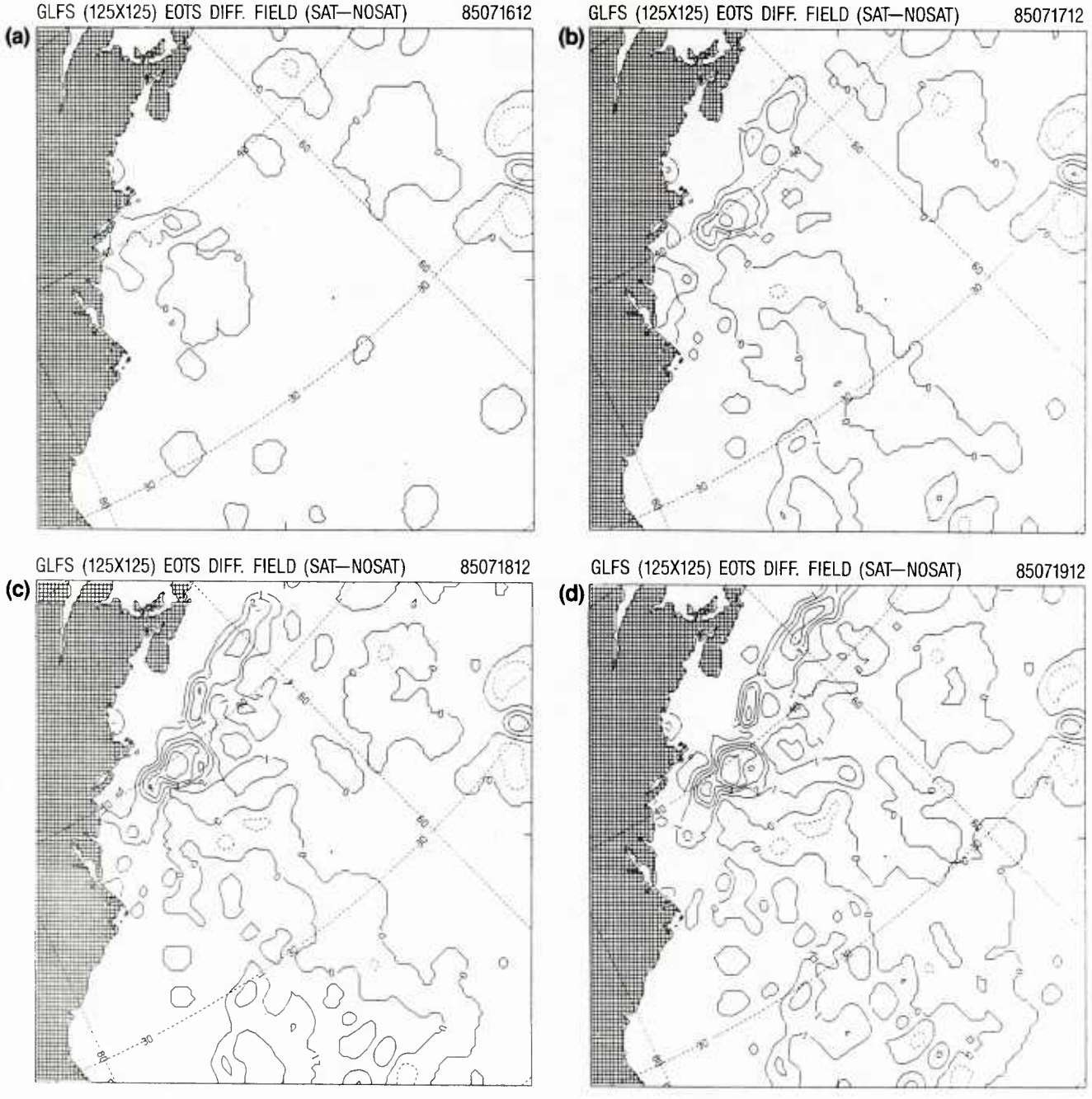

Figure 18. (a, b, c, d) Difference field between 20-km EOTS SST fields that include MCSST data and coincident ones without satellite SSTs for 12Z 16, 17, 18, and 19 July 1985.

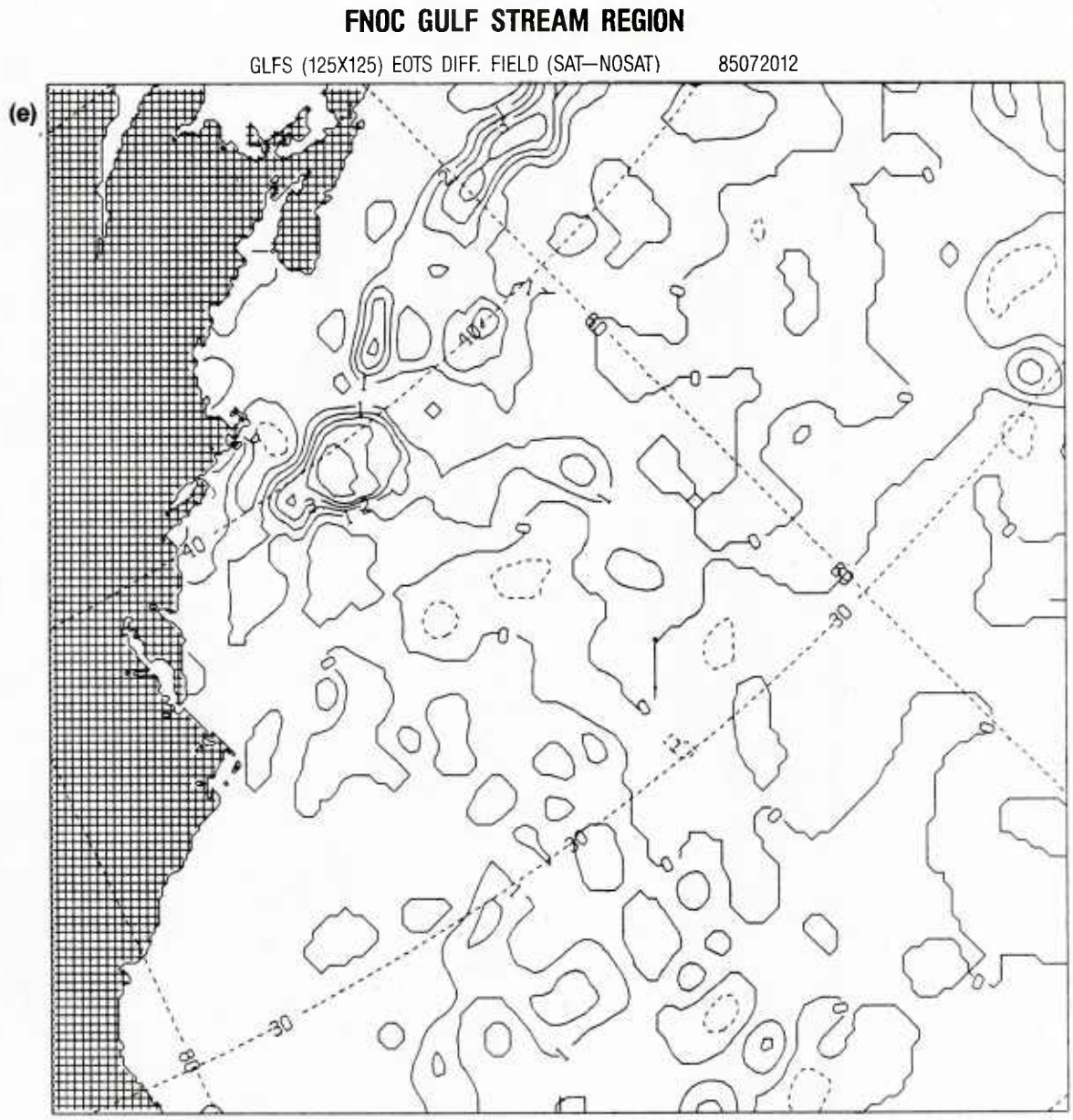

Figure 18. (e) Difference field between 20-km EOTS SST fields that include MCSST data and coincident ones without satellite SSTs for 12Z 20 July 1985.

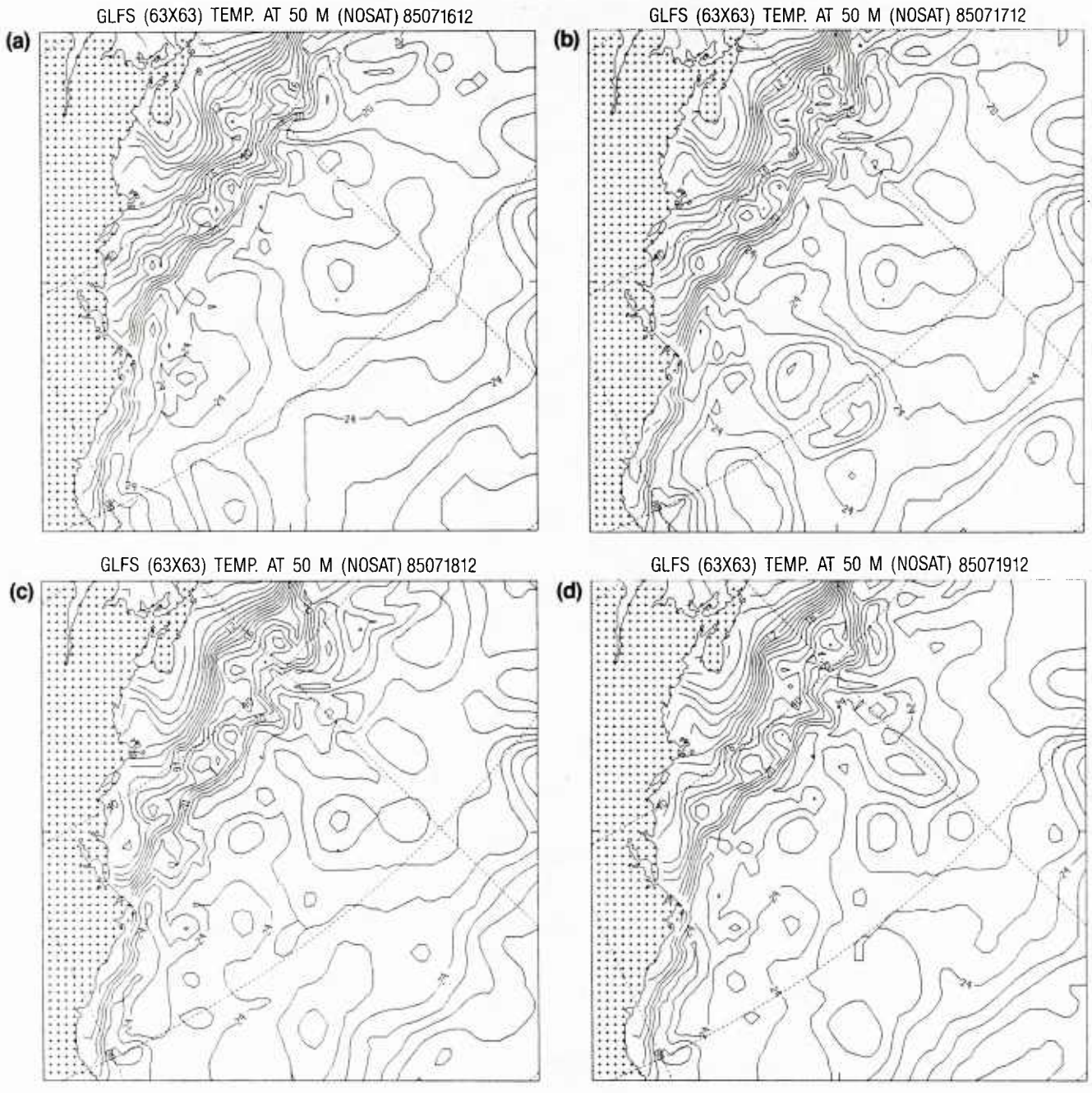

Figure 19. (a, b, c, d) EOTS 50-m temperature maps for 12Z 16, 17, 18, and 19 July 1985 without the use of MCSST measurements.

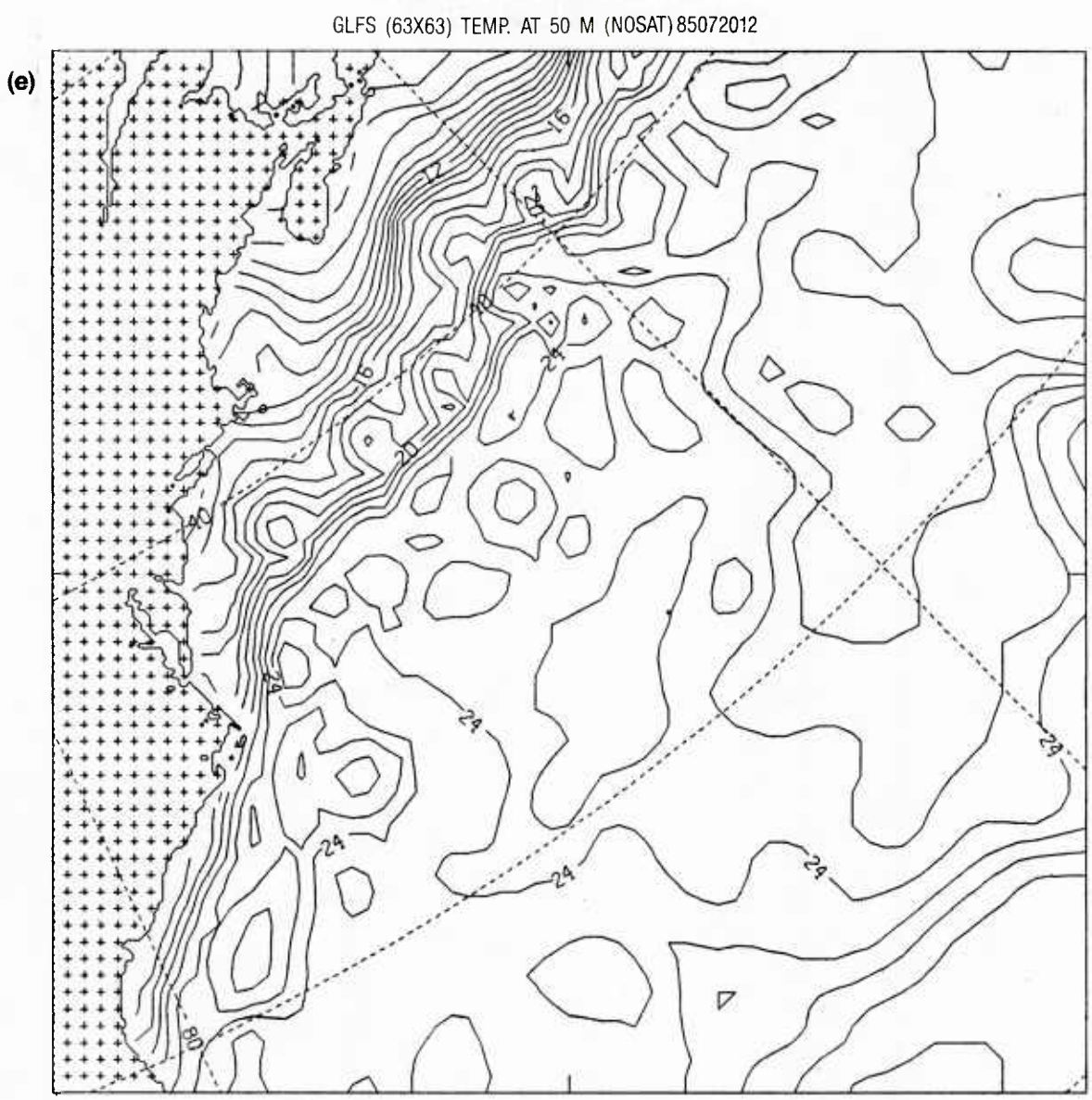

Figure 19. (e) EOTS 50-m temperature maps for 12Z 20 July 1985 without the use of MCSST data.

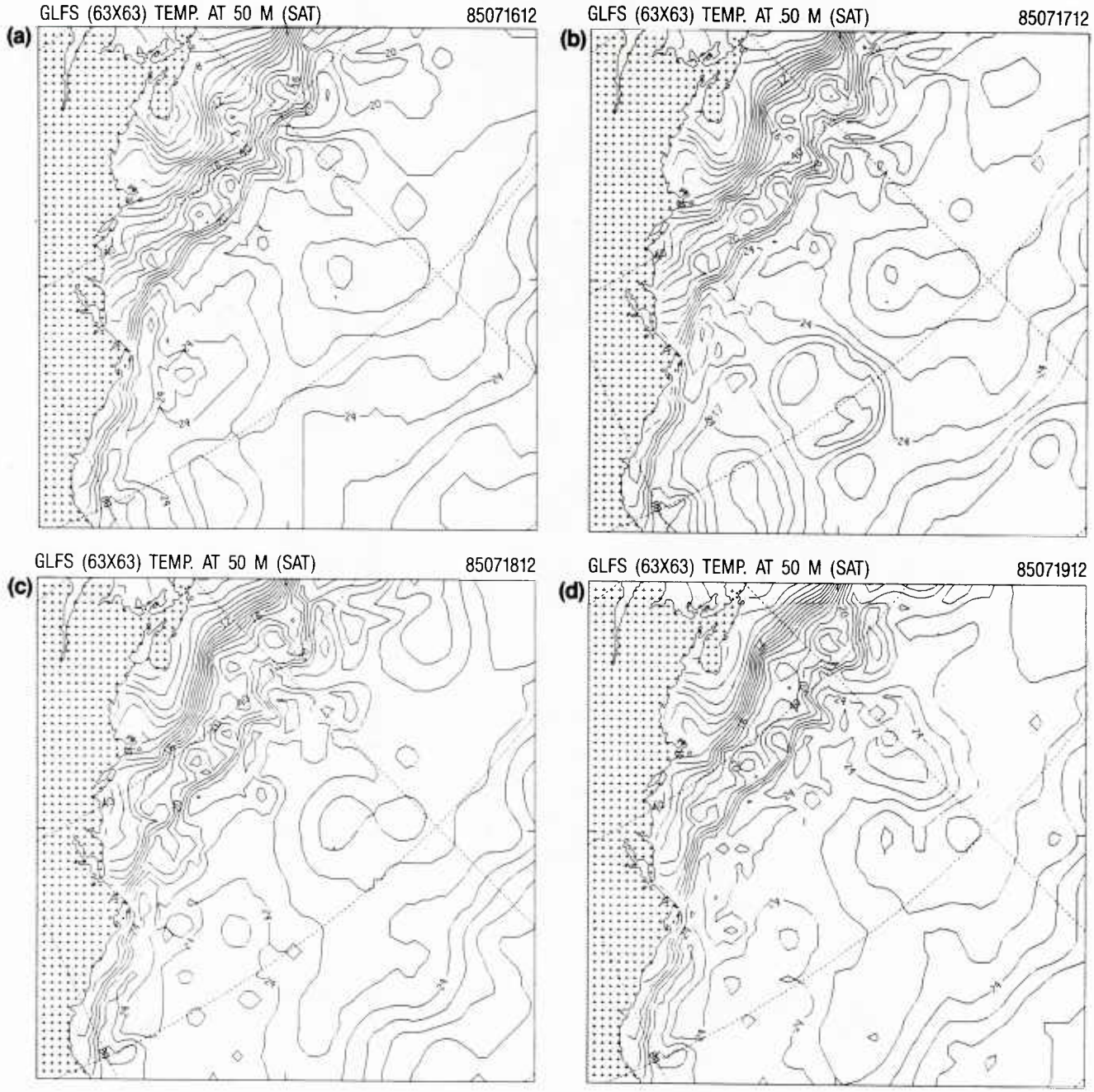

Figure 20. (a, b, c, d) EOTS 50-m temperature maps for 12Z 16, 17, 18, and 19 July 1985 with the incorporation of MCSST data.

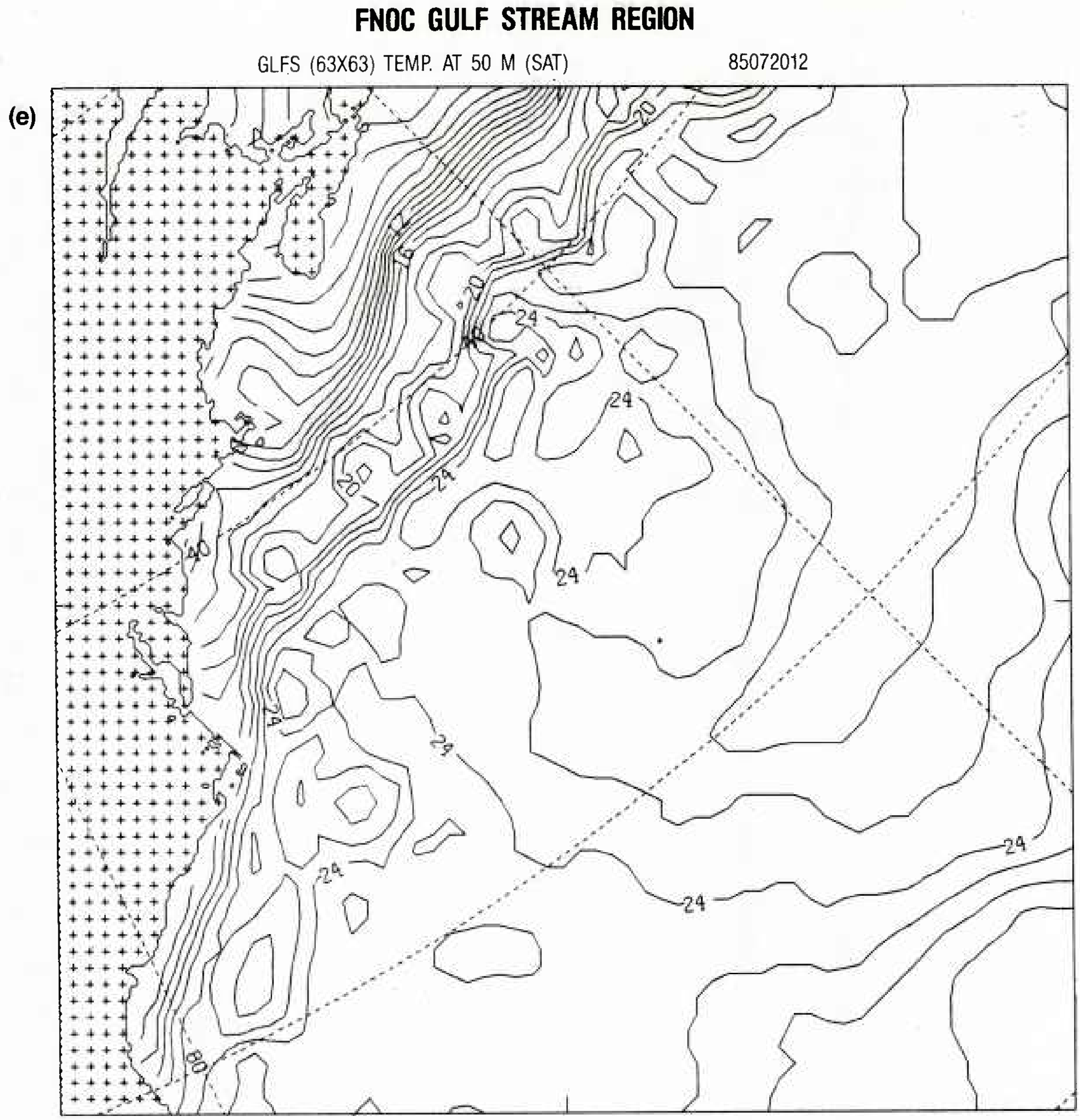

Figure 20. (e) EOTS 50-m temperature maps for 12Z 20 July 1985 with the incorporation of MCSST data.

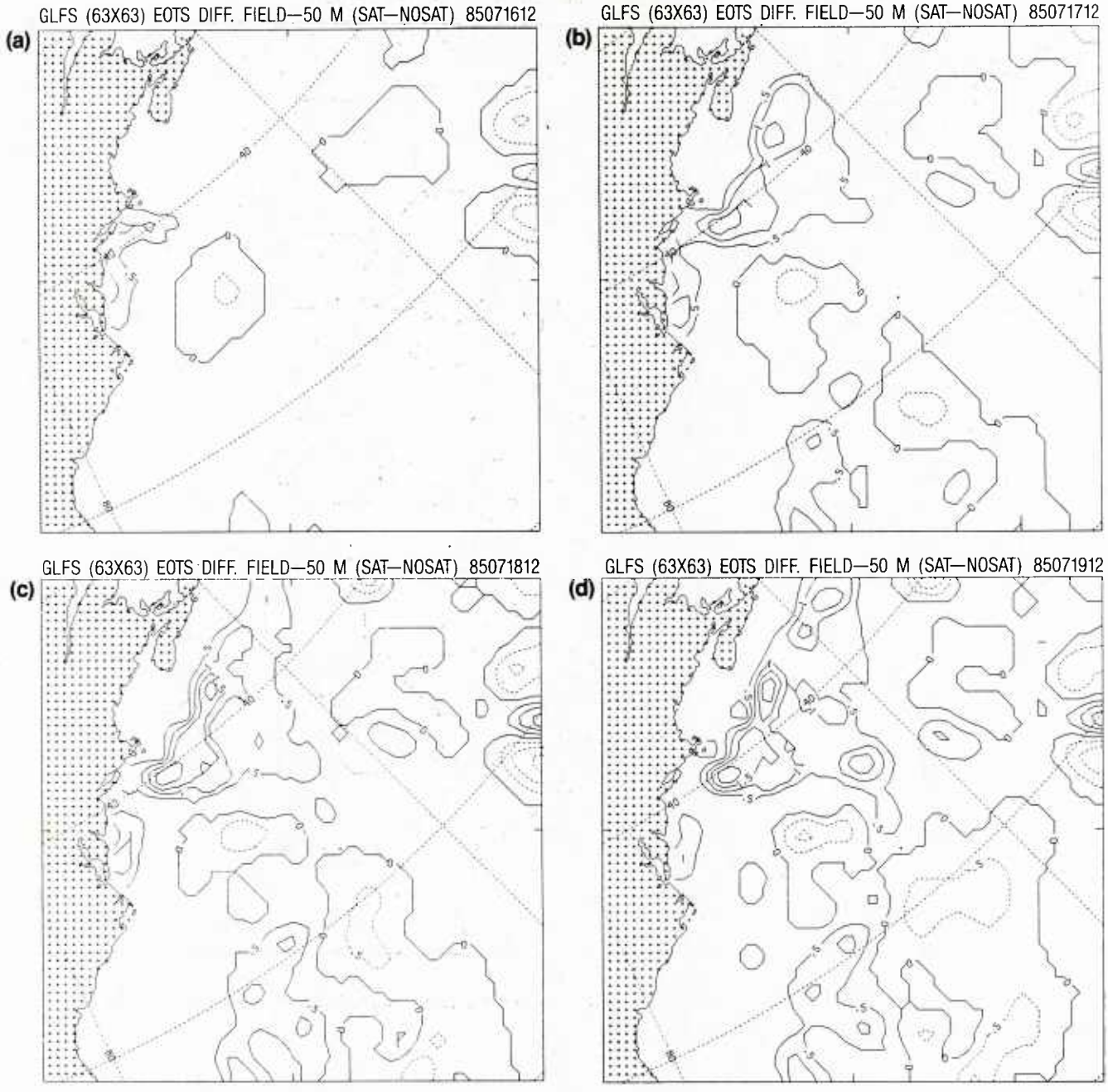

Figure 21. (a, b, c, d) Difference maps derived by subtracting the 50-m temperatures in the version not using MCSSTs from the EOTS run assimilating MCSSTs for 12Z 16, 17, 18, and 19 July 1985.

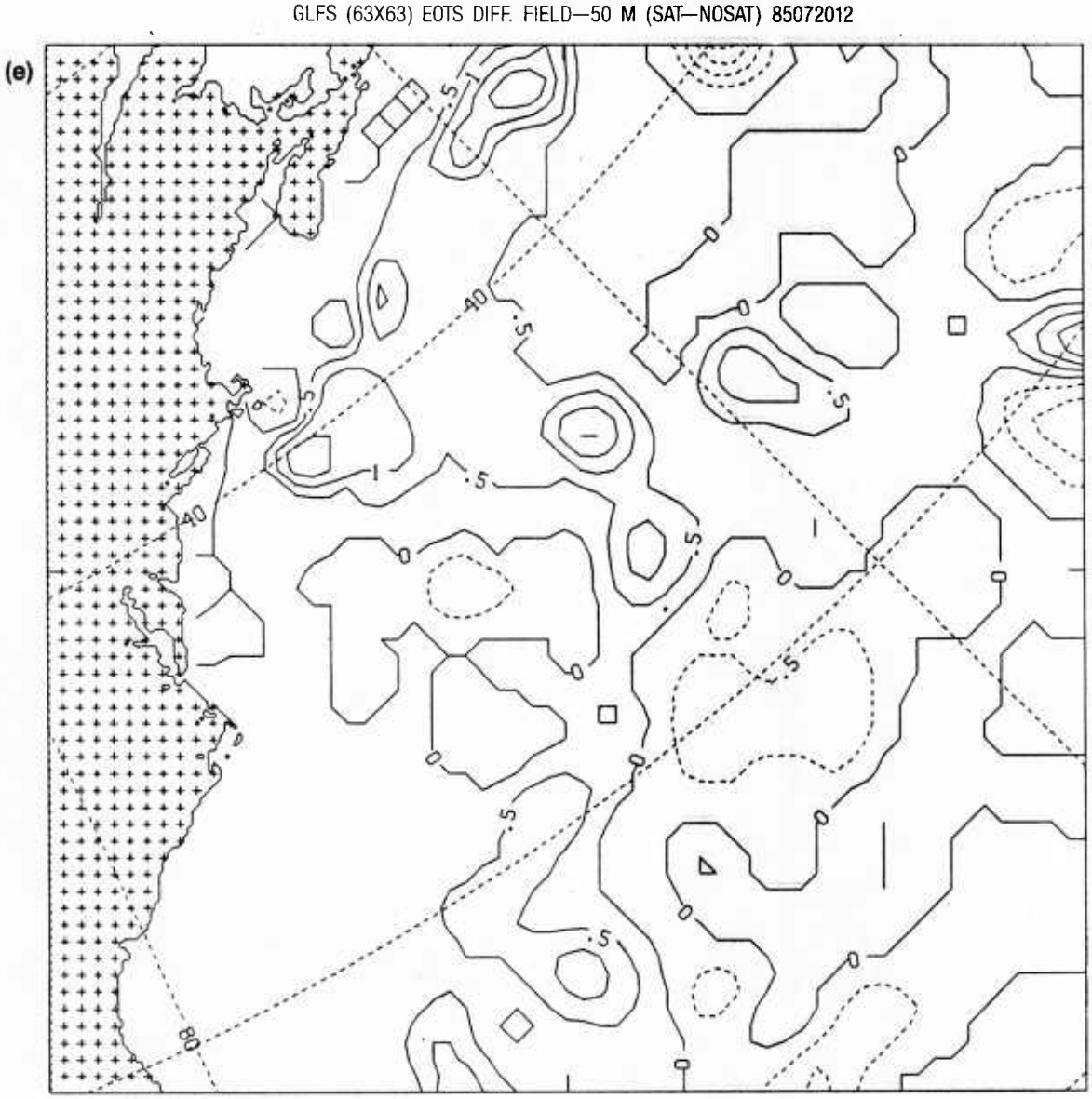

Figure 21. (e) Difference maps derived by subtracting the 50-m temperatures in the version not using MCSSTs from the EOTS run assimilating MCSSTs for 12Z 20 July 1985.